2020

Adakitic Paracale Granodiorite in southeastern Luzon, Philippines: A peek ata Proto-Philippine Sea Plate-related magmatic arc

Graciano P. Yumul Jr

Karlo L. Queaño

Jenielyn T. Padrones

Carla B. Dimalanta

Eric A. Andal

Journal of Asian Earth Sciences: X 4 (2020) 100035

Contents lists available at ScienceDirect

Journal of Asian Earth Sciences: X

journal homepage: www.journals.elsevier.com/journal-of-asian-earth-sciences-x

Adakitic Paracale Granodiorite in southeastern Luzon, Philippines: A peek at a Proto-Philippine Sea Plate-related magmatic arc

Graciano P. Yumul[a], Karlo L. Queaño[b], Jenielyn T. Padrones[c,*], Carla B. Dimalanta[d], Eric A. Andal[e,f]

[a] Cordillera Exploration Company, Inc., Bonifacio Global City, Taguig, Metro Manila, Philippines
[b] Department of Environmental Science, Ateneo de Manila University, Quezon City, Philippines
[c] Institute of Renewable Natural Resources, College of Forestry and Natural Resources, University of the Philippines – Los Baños, Laguna, Philippines
[d] Rushurgent Working Group, National Institute of Geological Sciences, College of Science, University of the Philippines, Diliman, Quezon City, Philippines
[e] Itogon-Suyoc Resources Inc., Itogon, Benguet, Philippines
[f] Apex Mining Co. Inc., Ortigas Centre, Pasig City, Metro Manila, Philippines

ARTICLE INFO

Keywords:
Adakitic rock
Paracale Granodiorite
Subduction zone
Proto-Philippine Sea Plate

ABSTRACT

This paper describes the geochemistry, petrogenesis and tectonic setting of a silicic pluton, the Paracale Granodiorite (PG), intruded into an ophiolitic suite in southeastern Luzon island, Philippines. Whole rock chemistry suggests that the PG samples are calc-alkaline and are characterized by light rare earth element (LREE)-enrichment and relatively weak heavy rare earth element (HREE)-depletion. They also show depletion in Nb, Ta, Zr and Ti and positive anomalies in K, Pb and Sr when normalized with the Primordial Mantle and normal-mid-ocean ridge basalt (N-MORB). The PG biotite mineral chemistry shows an affinity to calc-alkaline trends based on the FeO_{tot} versus Al_2O_3, whereas in the MgO-Al_2O_3 plot, they exhibit transitional calc-alkaline to peraluminous characteristics. These information, along with a temperature > 600 °C based on biotite chemistry, and hydrous setting for the generation of the PG suggest generation in a subduction-related setting. When plotted in the Y versus Sr/Y and Yb_N versus $(La/Yb)_N$, the PG samples exhibit adakitic signature. Partial melting, fluid addition and sediment participation are discerned from the geochemistry. Melting, assimilation, storage and homogenization (MASH) with limited fractionation are the dominant mechanisms of formation. The PG could represent a Late Cretaceous to Paleogene magmatic arc generated during the subduction of the proto-Philippine Sea Plate.

1. Introduction

Volcanic arc rocks, called adakites, are generated near trenches with the subduction of young hot oceanic crusts that have undergone slab melting (e.g. Defant and Drummond, 1990; Maury et al., 1996; Martin, 1999; Kamei, 2004). In areas where subduction initiation is recognized, adakites can also co-exist with boninites (e.g. Li et al., 2013; Cox et al., 2018). Nonetheless, a lot of volcanic rock suites that mimic the principal geochemistry of adakites (e.g. high Sr/Y, high La/Yb) would not be consistent with subduction-related slab melting in the forearc region. This has resulted into controversies on how adakites are generated (e.g. Defant et al., 2002; Richards and Kerrich, 2007; Moyen, 2009, Qian and Hermann, 2013). Thus, the use of the presence of adakites as a subduction-related forearc setting indicator needs to be re-examined. Silicic rocks (> 56% SiO2) that mimic adakites but would not be in sync with the original definition of adakites (*sensu lato* Defant and Drummond, 1990) have variably been called adakitic rocks, transitional adakites, intermediate adakites, adakite-linked andesites, adakite-like rocks or pseudo-adakites (e.g. Sajona et al., 2000; Eiler et al., 2007; Kamei et al., 2009; Castillo, 2012; Zhang et al., 2019). Other than near trench locations, adakitic rocks are also found in extensional within-plate settings, collision zones and thickened continental regimes (e.g. Ji et al., 2019; Temizel et al., 2019). Aside from slab-melting, lower crust melting, partial melting following delamination, assimilation-fractional crystallization (AFC) combined with melting, assimilation, storage and homogenization (MASH), high-pressure crystallization, sediment melting, mantle-melt hybridization, slab window melting, melting associated with flat slab subduction and magma mixing, to name a few, have been reported to explain the existence of adakites and adakitic rocks in non-forearc regions (e.g. Sajona et al., 1993; Martin et al.,

* Corresponding author.
E-mail address: jtpadrones@up.edu.ph (J.T. Padrones).

https://doi.org/10.1016/j.jaesx.2020.100035
Received 20 May 2020; Received in revised form 5 October 2020; Accepted 6 October 2020
Available online 17 October 2020

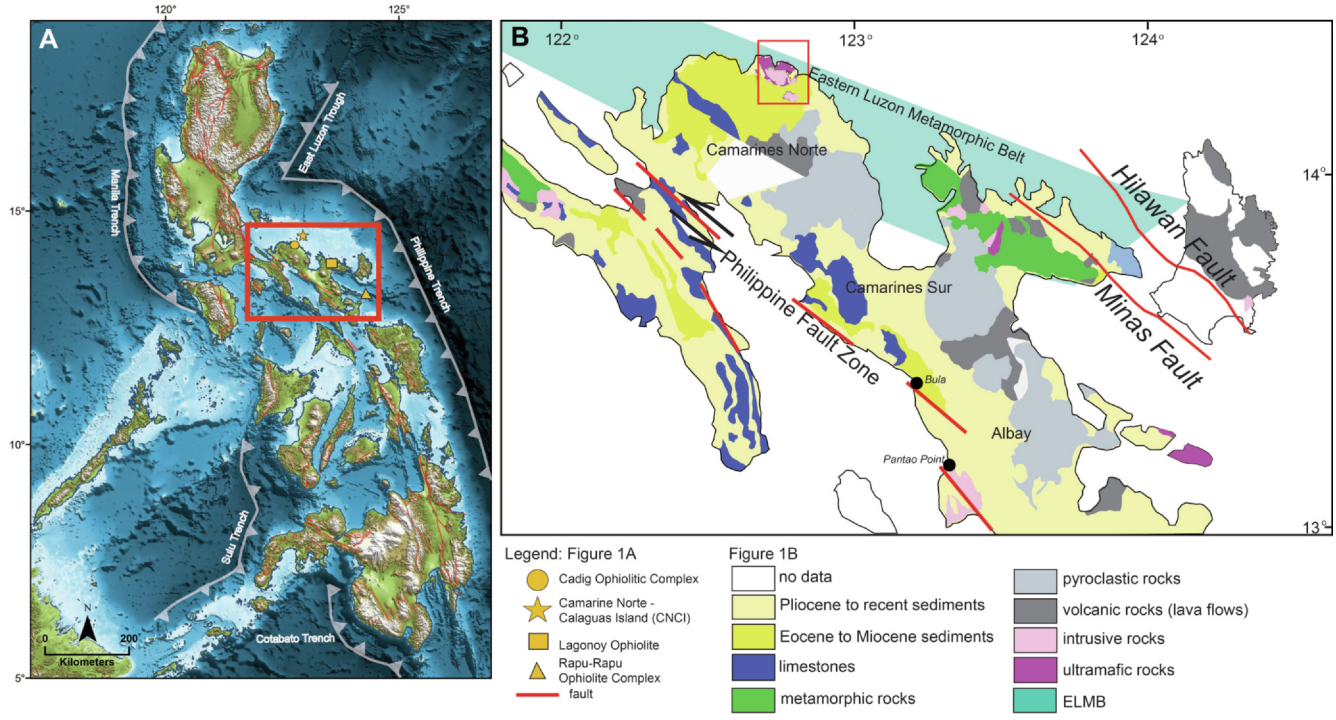

Fig. 1. (A) Tectonic map showing the location of the study area (red box). The location of the Cadig, Camarines Norte-Calaguas Island, Lagonoy and Rapu-rapu ophiolite complexes are also indicated. Map generated using topography and bathymetry data from Jarvis et al. (2008) and GEBCO 2019; (B) Location of the Paracale Mineral District (red box) in Camarines Norte. The Minas and Hilawan faults are also shown. The Camarines Norte, Camarines Sur and Albay provinces are all part of the Bicol Peninsula. Geologic map modified from MMAJ-JICA (1994). ELMB – Eastern Luzon Metamorphic Belt. (For interpretation of the references to colour in this figure legend, the reader is referred to the web version of this article.)

2005; Thorkelson and Breitsprecher, 2005; Macpherson et al., 2006; Moyen, 2009; Richards, 2011; Nakamura and Iwamori, 2013; Hu et al., 2017; Torkian et al., 2019; Hernandez-Uribe et al., 2020; Zhu et al., 2020).

In the Philippines, adakites and adakitic rocks (the latter term will be used to represent the two) are recognized in various settings that include forearc, main volcanic arc, and rift zones (e.g. Sajona et al., 1997; Bellon and Yumul, 2001; Yumul et al., 2003a; Jego et al., 2005). The mode of generation ranges from slab melting, lower crust melting, high-P fractionation, strike-slip faulting-related melting, assimilation-fractional crystallization, mantle-melt interaction, and ridge subduction (e.g. Castillo et al., 1999; Yumul et al., 2000; Ribeiro et al., 2016; Deng et al., 2017). The presence of adakitic rocks is also used as an exploration play marker as they are mostly found in areas characterized by precious-base metal mineralization (e.g. Sajona and Maury, 1998; Polve et al., 2007; Yumul et al., 2017; Deng et al., 2019). This has been recognized in the Paracale Mineral District which is one of the mining districts in the Philippines. It is located in the province of Camarines Norte, Bicol Peninsula, southeastern Luzon and hosts iron, nickel, gold and copper deposits (e.g. Comsti et al., 1985; Mitchell and Balce, 1990) (Fig. 1A). The gold deposits are mostly associated with the adakitic Paracale Granodiorite (PG). Unfortunately, there has been limited work done to understand the generation and evolution of the PG (e.g. Bryner, 1969; Giese et al., 1986; Mitchell, 1988). An understanding of the geology and geochemistry of the adakitic PG can help constrain its generation especially in the context of early magmatism in the Philippine archipelago with respect to the proto-Philippine Sea Plate evolution.

2. Geology

2.1. Regional geology

The NW-SE trending Bicol Peninsula is located in the southeastern part of Luzon island (Fig. 1A, B). Along with the other regions of the Philippine archipelago, this island has had a long history of subduction, collision and accretion of continental-derived sediments and ophiolitic fragments starting from the late Mesozoic to early Cenozoic (e.g. Karig, 1983; McCabe et al., 1985; Yumul et al., 2003b; Queaño et al., 2007, 2009). Arc formation and accretion events during the Cenozoic are mainly attributed to the interaction of the Philippine archipelago with the bounding plates, namely, the Philippine Sea Plate to the east and the Sunda Plate to the west (Yumul et al., 2008). Oblique subduction of these bounding plates is responsible for the formation of the left-lateral Philippine Fault Zone (Barrier et al., 1991; Rangin, 1991; Quebral et al., 1996).

The study area is within the Paracale Mineral District in the province of Camarines Norte located north of the Bicol Peninsula. The district is bounded by the NW-SE trending Philippine Fault Zone to the west and the west-dipping Philippine Trench to the east. In between these two active tectonic features are a series of NW-SE trending left-lateral faults, the Hilawan Fault and the Minas Fault, which David et al. (1997) consider as probable traces of the proto-Philippine Fault Zone (Fig. 1B). The district which lies to the west of the Minas Fault is floored by the Cadig Ophiolitic Complex (COC) which is correlated with the Jurassic to Cretaceous ophiolitic suites exposed in nearby areas (e.g. Geary and Kay, 1989; David et al., 1996; Tamayo et al., 2004) (Fig. 1A). Paleogene to Neogene intrusive rocks cut through the basement ophiolite suite (Mitchell and Balce, 1990; Encarnacion, 2004). Regionally- metamorphosed rocks, contact metamorphic aureoles related to intruded plutonic bodies, amphibolite soles associated with the emplacement of ultramafic bodies and chlorite-epidote schists intercalated with quartzo-feldspathic schist hosting volcanogenic massive sulfides are found throughout the Bicol Peninsula and adjoining islands (e.g. Mitchell et al., 1986; Geary et al., 1988; Sherlock et al., 2003; Yumul et al., 2006). Karig (1983) referred to these regionally-metamorphosed rocks as part of the NW-SE Eastern Luzon Metamorphic Belt (ELMB) that lies east of the Philippine Fault Zone (Fig. 1B). This metamorphic

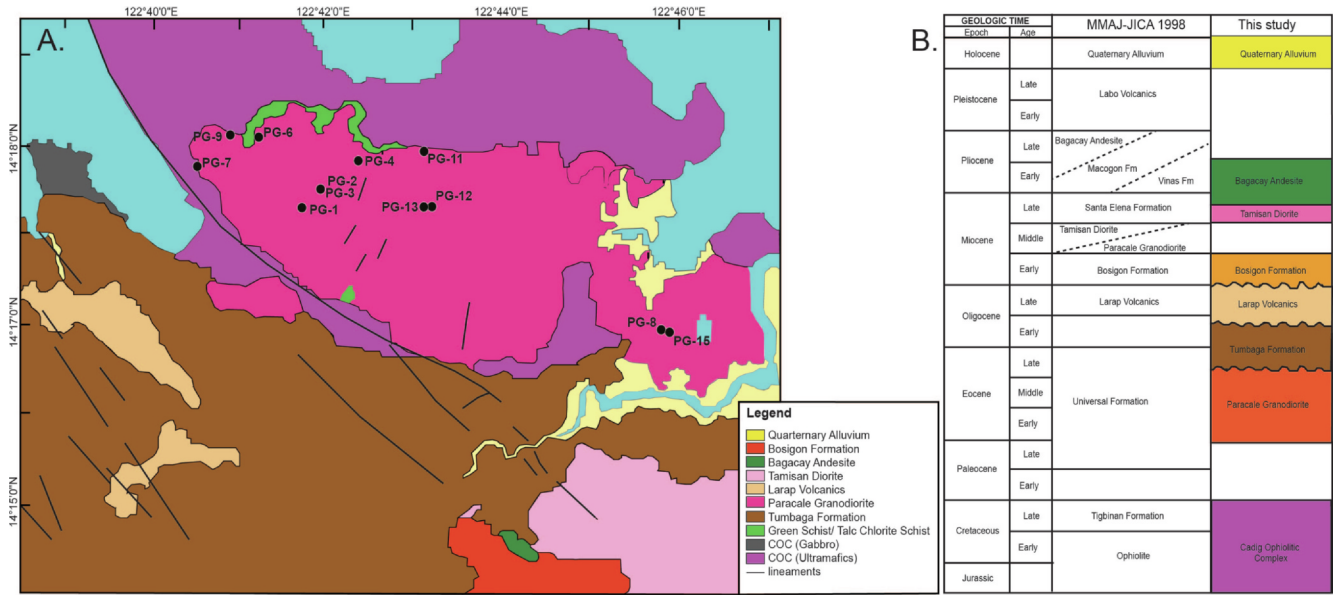

Fig. 2. (A) Geologic map of the Paracale Mineral District. Black dots with labels and numbers correspond to the samples analyzed in this work. (B) Stratigraphic column generated in this work compared with that of MMAJ-JICA (1998).

belt corresponds to the East Luzon-Samar-Mindanao disrupted terrane of McCabe et al. (1985). Unconformably overlying the metamorphic rocks are turbiditic clastic rocks, volcanic rocks and minor shallow-marine limestones. A NW-SE Pliocene to Recent volcanic arc characterizes the Peninsula. This young suite of volcanic arcs is related to the subduction of the Philippine Sea Plate along the Philippine Trench since the late Miocene – Pliocene time (e.g. Castillo and Newhall, 2004; Ozawa et al., 2004; Andal et al., 2005).

2.2. Local geology

In studying the PG, a 36-km^2 pluton, most of our field geological surveys were done within the Jose Panganiban-Paracale areas in Camarines Norte where most of the Au mines and Au-Cu prospects are present (Fig. 2A). The stratigraphy, from oldest to youngest, consists of: a.) Jurassic to Cretaceous COC; b.) Upper Eocene to Lower Oligocene Tumbaga Formation; c.) Oligocene Larap Volcanics and; d.) Lower Miocene Bosigon Formation. The PG and the Tamisan Diorite are the main intrusive bodies observed in the area (Fig. 2B). The pre-Tertiary COC is made up of harzburgites, dunites, layered ultramafic cumulates, isotropic gabbros, dike swarms, pillow lavas and breccias that are exposed mostly in the northern and coastal areas of Jose Panganiban and Paracale. The ophiolitic suite is best exposed in Cadig locality, thus, the use of this name (Fig. 3A–F). This ophiolitic complex serves as the basement in the area. The COC is correlative with the Jurassic to Cretaceous Camarines Norte-Calaguas Island Ophiolitic Complex and Lagonoy Ophiolite (e.g. Geary et al., 1988; Tamayo et al., 1996, 1998) (Fig. 1A). The Upper Eocene to Lower Oligocene Tumbaga Formation, formerly called the Universal Formation, is composed of a lower member of interbedded grayish to greenish sandstone and siltstone and few conglomerates, and an upper member of bedded marble. Coarser varieties (lithic sandstone and conglomerate) in western Jose Panganiban show mafic and quartz detritals as well as granule- to pebble-sized lithic fragments of peridotite and granodiorite. Silicification, chloritization and pyritization are noted in the vicinity of quartz veins intruded into the Tumbaga Formation. The compositional make-up of the Tumbaga Formation shows that the PG and the COC are the main sources of this formation. Contrary to earlier interpretations (e.g. MGB, 2010) that the Tumbaga Formation is older than the PG, this is not borne by our field observations. The Tumbaga Formation is thought to be either of Eocene or early Middle Miocene age (Miranda and Caleon, 1979 cited in Giese et al., 1986; Mitchell and Balce, 1990). The Oligocene Larap Volcanics, on the other hand, is made up of massive porphyritic andesite to layered andesite oriented N55W/65SW. The Lower Miocene Bosigon Formation consists of light gray, fine- to medium-grained arkosic sandstone that is slightly magnetic. Associated conglomerates with clasts of mostly andesite porphyry and minor limestone set in a grayish, calcareous matrix are observed. The clastic rocks are underlain by calcareous, bedded, fine- to medium-grained sandstone and grayish limestone. The PG comprises roughly the central portion of the Jose Panganiban-Paracale area, oriented approximately in a WNW-ESE direction and surrounded mostly by peridotites. This unit consists of quartz and plagioclase, with subordinate amounts of biotite, relict pyroxenes and opaque minerals. The granodiorite, in many places, is metamorphosed, being in transition to quartz-feldspar schists and are most prominent near the contact with the peridotites (Fig. 4A–C). Gneissic texture and a foliation trend of NW-SE are noted. The PG is intrusive into the COC. Gabbro, peridotite and chlorite schist xenoliths are found within the granodiorite. Various ages have been assigned to the granodiorite, ranging from Paleocene to Pleistocene (Frost, 1965). A K-Ar dating of samples (biotite extract) provided a range of ages from 14.4 Ma (Giese et al., 1986) to 18.6 Ma (Geary et al., 1988), pointing to a late Early Miocene to early Middle Miocene age. The Miocene age may actually represent the last metamorphic event as will be expounded later. As noted, granodiorite clasts are present in the Late Eocene to Early Oligocene Tumbaga Formation. The Late Miocene (hornblende K-Ar age date of 6.96–10.6 Ma) Tamisan Diorite is a classic “salt and pepper” type, with an almost equal felsic (feldspar + quartz) and mafic (mainly hornblende) components (MGB, 2010) (Fig. 4D). The diorite is slightly to moderately magnetic, although silicified varieties rarely exhibit such property.

3. Methodology

Representative fresh to weakly-altered granodiorites were selected for geochemical analysis. The samples were powdered using an agate ball mill and mortar and pestle. The whole rock major oxide compositions were analyzed using the Panalytical Axios Max X-ray fluorescence spectrometer at the Bureau Veritas Mineral Laboratories in Canada. The whole rock trace element concentrations were derived using the Inductively Coupled Plasma-Mass Spectrometer (ICP-MS) ELAN 9000 also of the Bureau Veritas Mineral Laboratories in Canada. The

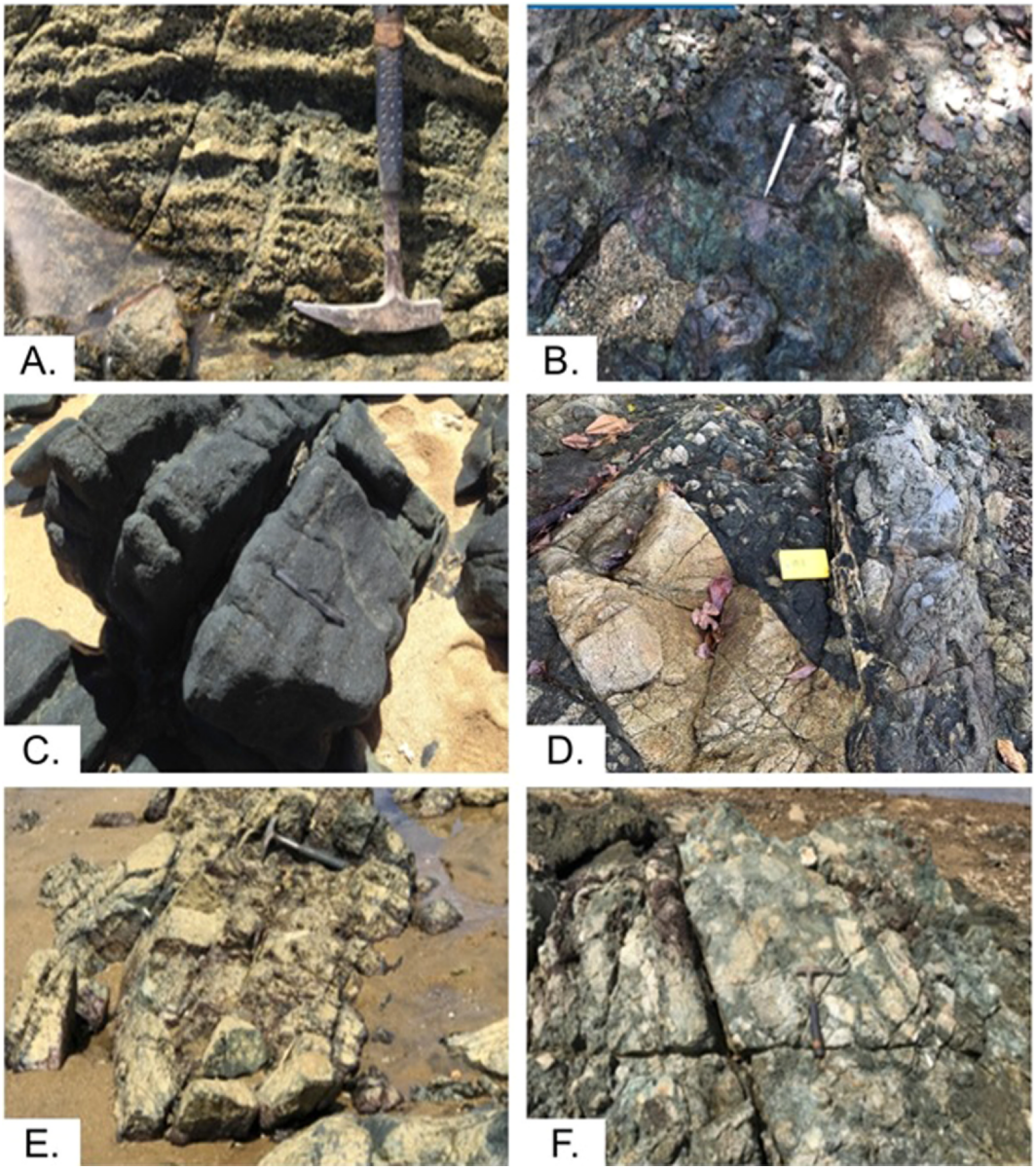

Fig. 3. Outcrop photos of the Cadig Ophiolitic Complex (COC). (A) Layered gabbro, (B) Pillow lavas, (C) Layered ultramafic rocks, (D) Dike swarm, (E) Harzburgite, (F) High-level gabbro containing gabbro and diabase clasts.

analytical precision of the data based on replicate samples is less than 1% for the major oxides and up to 10% for the trace elements. The major oxide and trace element compositions are listed in Supplemental Table (ST) 1. Double-polished thin sections of the rock samples were prepared for petrography and mineral chemistry analyses. Selected thin sections were carbon coated using the 108C Auto Carbon Coater to increase surface conductivity. Mineral chemistry of the granodiorites and the ultramafic rocks were obtained using the JEOL JXA-8230 Electron Probe Micro Analyzer at the University of the Philippines-National Institute of Geological Sciences. Wavelength dispersive X-ray spectroscopy (WDS) analysis was utilized to identify the major oxide compositions of mineral grains. The plagioclase and biotite of the granodiorite and olivine and magnetite of the ultramafic rocks were analyzed using a probe diameter of 3–5 μm at 15 kV acceleration voltage, 20 nA current and 15 μm probe diameter. ZAF correction was applied to account for the atomic number, absorption and fluorescence correction. Mineral standards used were from Astimex Standard Limited. Major oxide compositions of representative minerals are listed in ST 2A-D.

4. Results

4.1. Petrography

The PG are coarse grained, leucocratic rocks that are distinctly foliated. In thin section, the main constituents are subhedral to euhedral plagioclase (40–60% mostly oligoclase) and subhedral quartz (30 to 50%) (Fig. 4E, F). The plagioclase is often twinned, zoned and with resorbed boundaries, while the quartz commonly displays undulatory extinction. Minor occurrences of biotite (2–10%) and epidotes (< 2%) are noted. Although of minor amount, the alignment of biotite defines the foliation trend (generally directed NW) of the granodiorite. While it was not encountered in this study, K-feldspar (1–2%) in granodiorites were previously reported by Giese et al. (1986). In terms of the ultramafic rocks, the dunites and harzburgites are affected by varying degrees of serpentinization. Protogranular olivine (65–90%) is a common constituent that shows indications of serpentine replacement along crystal boundaries or within the crystal itself (in this case, indicated by a network of cross-cutting serpentine veins). Orthopyroxenes (10–30%)

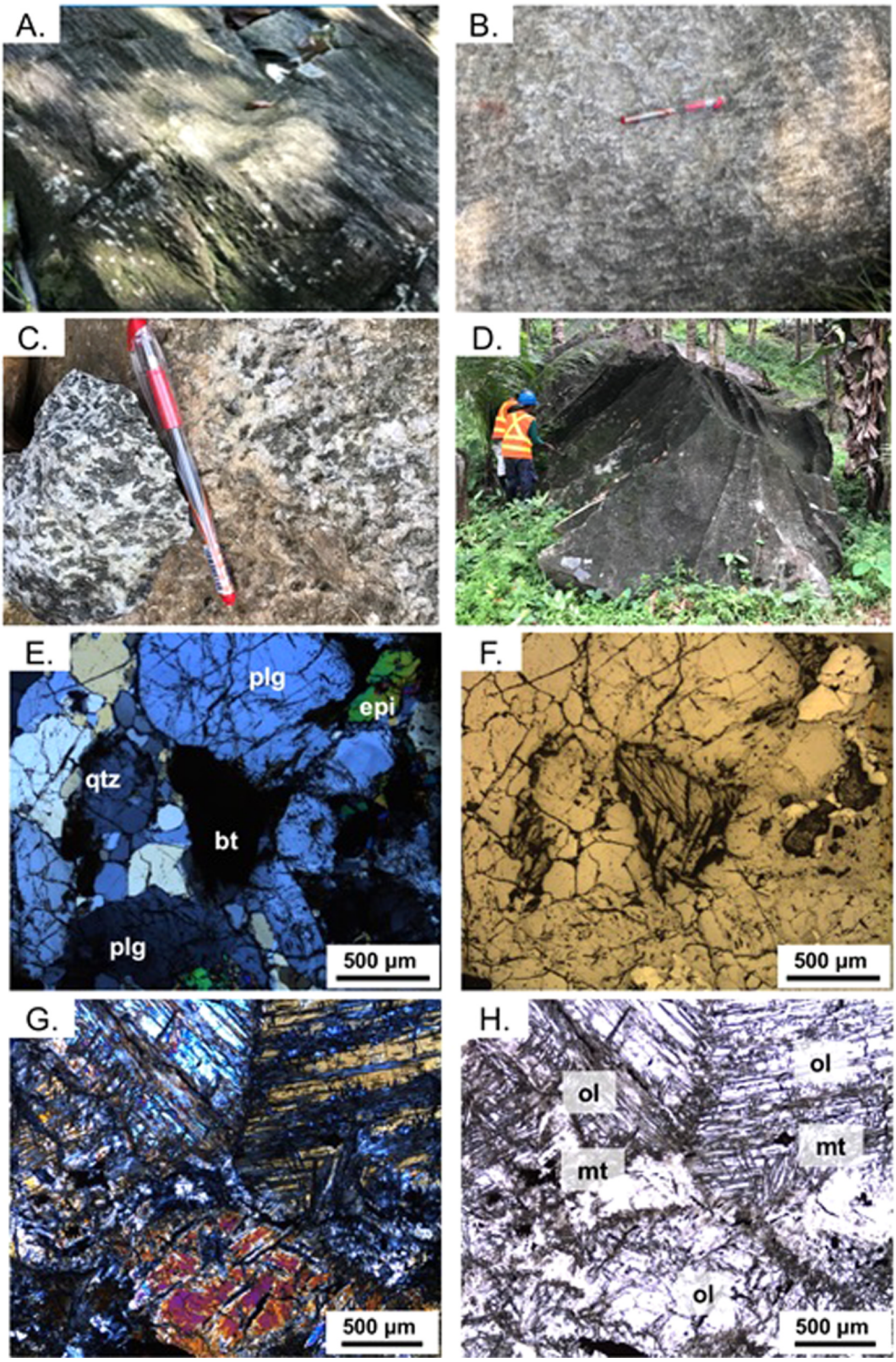

Fig. 4. Outcrop photos of the Paracale Granodiorite (A–C) and Tamisan Diorite (D). Photomicrographs of a granodiorite (E,F) and COC dunite (G,H) sample (crossed and uncrossed polars).

are not prominent being commonly altered to bastite. Deformation of the ultramafic rocks is made obvious by the kinking of serpentine grains as well as the undulose extinction of olivine. Common accessory minerals are anhedral magnetites (Fig. 4G, H). Fine-grained, chromium-rich, red-brown and aluminum-rich green spinels in the ultramafic rocks have been reported (Geary and Kay, 1989).

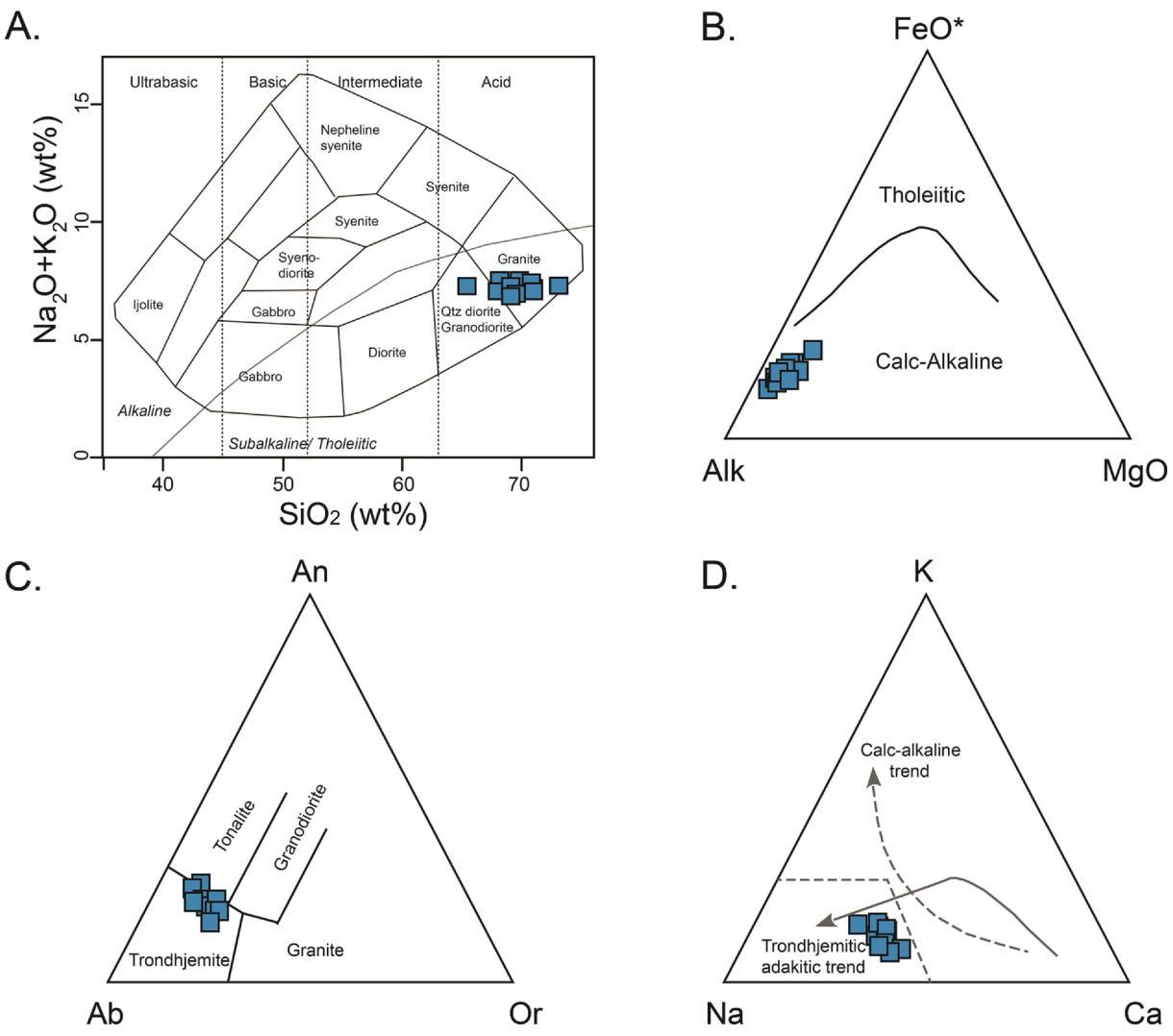

Fig. 5. (A) SiO_2 vs Na_2O + K_2O (wt%) plot reveals granite and granodiorite composition of the PG samples. (B) AFM diagram displays the calc-alkaline affinity of the PG samples. (C) An-Ab-Or and (D) K-Na-Ca plots show that most PG samples are trondhjemites.

4.2. Whole rock chemistry

Whole rock chemical analysis shows that most of the PG cluster in the 65–72 wt% SiO_2 range (ST 1). Although within a limited range, with increasing SiO_2, the PG exhibits a decrease in Al_2O_3, MgO, FeO_{tot}, TiO_2, CaO, P_2O_5, MnO and to a certain extent, Na_2O and Cr_2O_3. For trace elements, with increase in SiO_2, there is a decrease in Sr, Sc, Y, V, Co, Cu, the rare earth elements (REEs) and, although not so clear, in Ni and Hf (SF 1A-H). Increase in K_2O, Ba and Cs as SiO_2 increases is noted among the PG samples. The SiO_2 versus Na_2O + K_2O diagram shows that the PG plots in the granite and quartz diorite (granodiorite) fields consistent with its acidic composition (Cox et al., 1979; Le Bas et al., 1986) (Fig. 5A). On the other hand, the Nb/Y versus Zr/TiO_2 has the PG in the rhyolite to dacite fields (Winchester and Floyd, 1977) (SF 2A). All PG samples in the AFM diagram exhibit medium-K calc-alkaline affinity (Irvine and Baragar, 1971; Peccerillo and Taylor, 1976) (Fig. 5B; SF 2B). Normative compositions (An-Ab-Or) display that almost all of the PG are trondhjemites (Fig. 5C). The PG does not follow the typical calc-alkaline trend towards K-enrichment but more of the trondhjemitic/adakitic trend in the K-Na-Ca diagram (Martin, 1999) (Fig. 5D). All of the PG are I-type, weakly peraluminous in the A/CNK (mol. ratio) versus A/NK (mol. ratio) (Fig. 6A) (Maniar and Piccoli, 1989; Chappell and White, 1974, 2001). The PG samples plot in the volcanic arc granite (Y + Nb versus Rb) to volcanic arc granite plus *syn*-collisional granite (Y versus Nb) fields and have no affinity with anorogenic granites (10^4 Ga/Al versus Zr) (Pearce et al., 1984; Whalen et al., 1987) (Fig. 6B,C; SF 3). In the Y versus Sr/Y and Yb_N versus $(La/Yb)_N$ diagrams, the PG plots in the adakite field (Defant and Drummond, 1990; Martin, 1999) (Fig. 7A,B) (Table 1; ST 1).

4.3. Rare earth elements

The PG samples (REE = 1–100x chondrite) exhibit a spoon-shaped trend and are characterized by light rare earth element (LREE)-enrichment and relatively weak heavy rare earth element (HREE)-depletion. The PG samples show depletion in Nb, Ta, Zr and Ti and positive anomalies in K, Pb and Sr when normalized with the Primordial Mantle and normal-mid-ocean ridge basalt (N-MORB). No Eu anomaly is observed (Sun and McDonough, 1989) (Fig. 8A,B; SF 4). The REE trend of the PG exhibits depletion in the middle rare earth elements (MREEs). The subtle decrease in Gd/Yb as SiO_2 increases, though of limited range, is consistent with this (Hildebrand and Whalen, 2014) (Fig. 9A). Partial melting is the dominant process as suggested by the La_N versus $(La/Yb)_N$ diagram (Lin et al., 1989) (Fig. 9B). The La/Sm has a limited range whereas an increase in Sm/Yb (from 2 to 5) can be noted. The La/Sm (4–8) vs Sm/Yb (2–5) is consistent with extraction from a source that has pyroxene and amphibole remaining in the residue (Kay and Mpodozis, 2001) (Fig. 9C). The PG samples are more consistent with

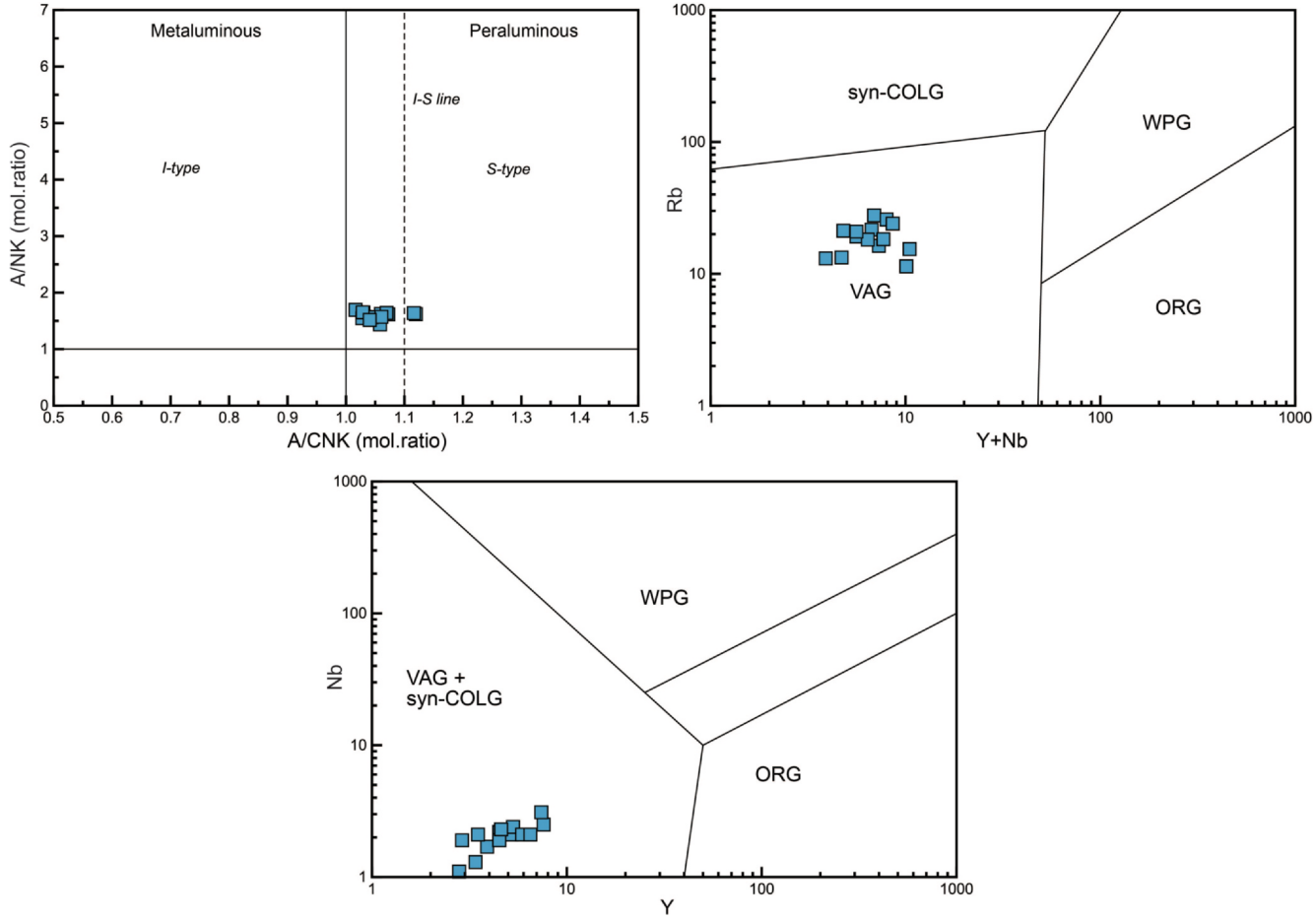

Fig. 6. (A) A/CNK vs A/NK diagram conveys peraluminous and intermediate I-S type classification for the PG samples. (B) Y + Nb vs Rb and (C) Y vs Nb plots manifest affinity of the PG samples with the Volcanic Arc Granite (VAG) and *syn*-collisional (*syn*-COLG) tectonic settings. Legend: WPG – Within Plate Granite, ORG – Ocean Ridge Granite.

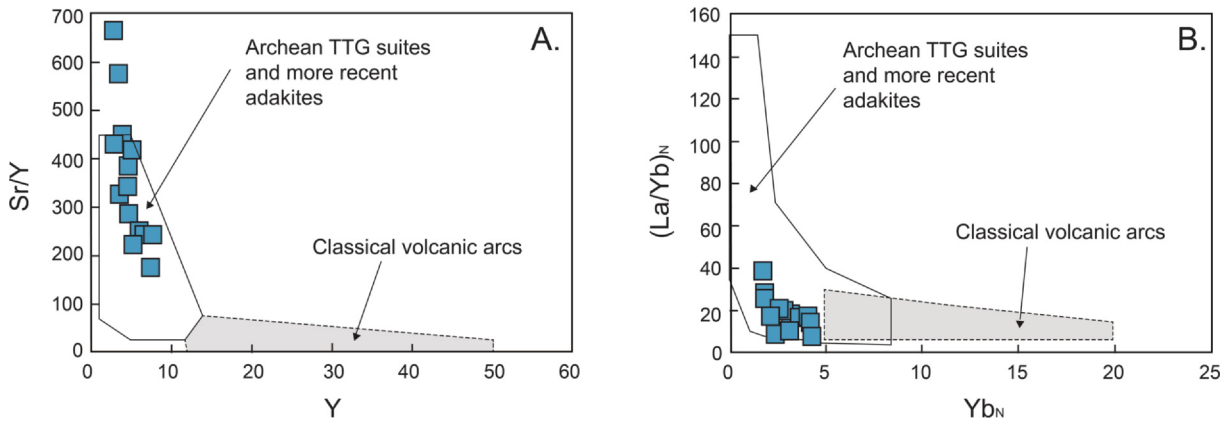

Fig. 7. A. Y vs Sr/Y and B. Yb_N vs $(La/Yb)_N$ plots reflect the adakitic signature of the PG samples.

partial melting products of subducted oceanic crust rather than lower continental crust as displayed in the $(La/Yb)_N$ versus Sr/Y (Xue et al., 2017) (Fig. 9D).

4.4. Mineral chemistry

The PG is composed of quartz, plagioclase, biotite and minor epidote and magnetite. The feldspars are albitic. The cores and rims of the PG plagioclases are dominantly oligoclase (Ab70-89, An11-28, Or1-2) and no reverse zoning is noted (Fig. 10A,B; ST 2A). The PG biotites plot in the biotite field of the Al_{tot} versus Fe(Fe + Mg) diagram (Foster, 1960; Deer et al., 1996; Rieder et al., 1998; Karimpour et al., 2011, Moradi et al., 2016) (Fig. 11A). The FeO_{tot} (20.5–22.4 wt%), MgO (11.1–12.6 wt%), TiO_2 (1.8–2.4 wt%), Al_2O_3 (15.0–15.7) and MnO (0.32–0.40) classify the biotite as primary to reequilibrated biotites in the $10(TiO_2)$ – FeO + MnO – MgO diagram (Nachit et al., 2005) (Fig. 11B). Furthermore, the FeO_{tot} versus Al_2O_3 displays the biotites as having an affinity to calc-alkaline melts (Abdel-Rahman, 1994) (Fig. 11C; ST 2B). The PG biotites when plotted in the MgO-FeO-Al_2O_3 demonstrate affiliation with calc-alkaline orogenic suites whereas in the

Table 1
Geochemical characteristics of adakites compared with those of Paracale Granodiorite. Adakite characteristics are compiled from Defant and Drummond (1990), Kamber et al. (2002), Castillo (2012), Eiler et al. (2007), and Zhang et al. (2019).

Adakite	Paracale Granodiorite
SiO_2 > 56 wt%	65–72 wt%
Al_2O_3 ≥ 15 wt%	15–19 wt%
MgO < 3	0.3–1.1 wt%
Na2O > 3.5 wt%	5–6 wt%
Ni < 24 ppm	2–19 ppm
Y ≤ 18 ppm	2.8–7.6 ppm
Yb < 1.9 ppm	0.2–0.7 ppm
Sr > 400 ppm	1150–2180
K_2O/Na_2O ~ 0.42	0.20–0.41
Sr/Y > 40	150–450
La/Yb > 20	8–40
Zr/Sm > 50	47–127
Pb/Nd < 0.40	0.04–0.25; 2.5–3.0
Nb/Ta > 15	10–23
Mg#	51–66
No Eu anomaly	None

MgO- Al_2O_3 plot, the biotites exhibit transitional calc-alkaline to peraluminous characteristics (Abdel-Rahman, 1994) (SF 5A,B). Table 2, however, shows the dominant similarity of the PG with the calc-alkaline suites. A temperature range of 600–650 °C is observed in the Mg/Mg + Fe versus Ti of Henry et al. (2005) (Fig. 11D).

Almost all of the ultramafic rocks in the COC had undergone serpentinization. Massive to layered harzburgites, dunites and clinopyroxenites are present (Fig. 3). Olivine that has escaped serpentinization is forsteritic showing a narrow range of Fo# [(100 × Mg/(Mg + Fe_{tot})] 86–89 (Fig. 12A; ST 2C). Olivine has a MnO range of 0.14–0.37 wt% whereas NiO ranges from 0.24 to 0.37 (Fig. 12A, B). A lot of the dunites plot within the olivine mantle array (e.g. Takahashi, 1986; Arai et al., 2018). However, an equal number of the dunites and harzburgites plot below the olivine mantle array, too. As Fo# decreases, NiO decreases whereas MnO increases. On the other hand, no chromian or aluminian spinel is present among the ultramafic rocks of the COC. The spinels are all magnetites with YFe^{3+} [$Fe^{3+}/(Cr^{3+}+Al^{3+}+Fe^{3+})$] 91–99, YCr^{3+} [$Cr/(Cr^{3+}+Al^{3+}+Fe^{3+})$] 2–13.5, YAl^{3+} [$Al/(Cr^{3+}+Al^{3+}+Fe^{3+})$] 0–0.25 (Haggerty, 1991; Barnes and Roeder, 2001; Gargiulo et al., 2013) (Fig. 12C, SF 6; ST 2D).

5. Discussion

5.1. Paracale Granodiorite: An orogenic calc-alkaline rock suite

The PG exhibits a limited range of SiO_2 with quartz and plagioclase as the major crystallizing phases, and biotite, apatite, oxide and titanite minerals as accessory minerals. The decrease in Mg, Ca, Fe, Ti, P, and Sc as fractionation progresses is consistent with this (SF 1). In addition, the whole rock chemistry of PG exhibits calc-alkaline character which is further reinforced by the plots in the modified aluminum-lime index versus SiO_2(MALI: Na_2O + K_2O-CaO) and SiO_2 versus FeO_{tot}/(FeO_{tot} + MgO) (Frost et al., 2001; Frost and Frost, 2008) (Fig. 13A,B). Such plots also show magnesian signatures for the PG.

Although the whole rock chemistry of PG exhibits calc-alkaline character, the samples have more affinity with the trondhjemites – adakites (Fig. 5C,D). The PG is of the volcanic-arc granite type consistent with a subduction-related setting (Fig. 6B,C) (e.g. Pearce et al., 1984). The PG can be further classified as I-type, consistent with its affinity to the magnetite-series granites (Ishihara, 1977).

Interestingly, the geochemical plots also suggest that PG is somewhat peraluminous (Fig. 6A). While only weakly exhibited, such peraluminous characteristic of the PG cannot be discounted. As a note, peraluminous granites are usually formed in within plate settings, extensional regimes or areas that have undergone crustal delamination (e.g. Barbarin, 1999; Frost et al., 2001). There is no field evidence, however, to suggest that the PG was generated in a within plate setting–related rift regime.

It has been suggested that crustal or sediment melting plays a role in the generation of peraluminous granites (Chappell and White, 2001). This is the case for the generation of PG based on its high Th (0.5–1.9 ppm) and Zr (68–121 ppm) content. The Ta/Yb versus Th/Yb shows that the PG has active continental margin and within plate volcanic zone geochemical character which accounts for the role played by sediments during magma generation (Pearce, 1982) (Fig. 13C). The high Zr/Y (11–36) of the PG also signifies a sediment component, possibly of continental derivation, in its generation (Pearce and Norry, 1979) (Fig. 13D).

The limited range of the PG in terms of SiO_2 makes it difficult to determine a clear fractionation trend. The plagioclase data, though, demonstrate that no magma mixing happened. All the oligoclase cores and rims show the same range of composition (Fig. 10). In addition, the presence of biotite indicates a hydrous setting for the PG (e.g. Wones and Eugster, 1965; Wones, 1981; Luhr et al., 1984). Although the PG biotites range from primary to reequilibrated, almost all of them exhibit distinct orogenic suite-related calc-alkaline affinity (Fig. 11B,C; SF 5A,B). The MgO of biotite in the calc-alkaline suites is 7–19 wt% as compared to the 2–8 wt% of peraluminous rock suites (Abdel-Rahman, 1994). The PG biotite MgO has a limited range of 11–12.6%, again consistent with its calc-alkaline affinity. However, the PG biotites are also characterized by high Al_2O_3 and low TiO_2 which could account for the weak peraluminous and ilmenite-series signatures they have (SF 5B; SF 7A). The low TiO_2 could be attributed to a.) the retention of a titanate mineral in the source region thus lowering the TiO_2 content of the melt, b.) the rock suite being subduction-related which is typically characterized by low TiO_2 content or c.) formation in an environment characterized by low temperature and low oxygen fugacity (Henry

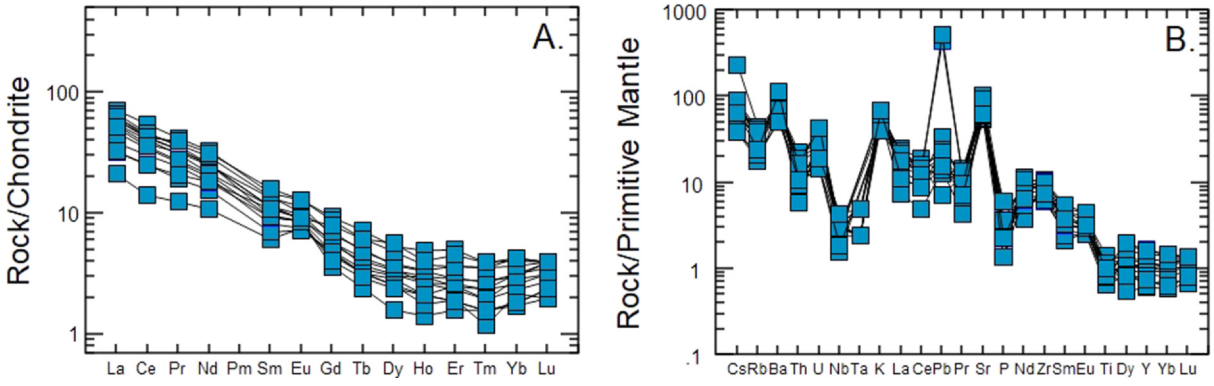

Fig. 8. Multi-element diagrams normalized to A. chondrite and B. primitive mantle. Normalizing factors from Sun and McDonough (1989).

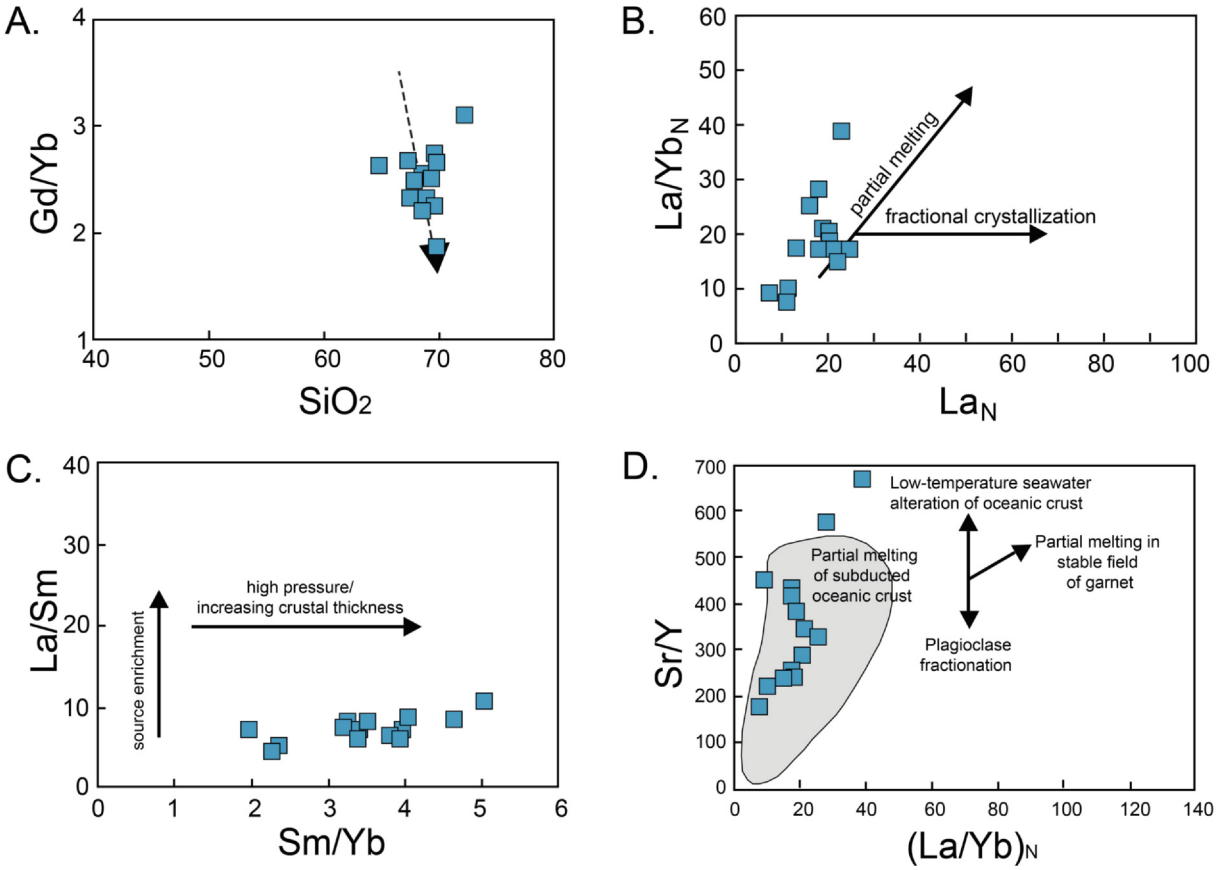

Fig. 9. (A) The PG samples show decrease in Gd/Yb with increasing SiO_2. (B) Partial melting of PG samples as the major process compared to fractional crystallization is indicated in the La_N vs La/Yb_N plot. (C) Sm/Yb vs La/Sm plot suggests the important role of amphibole crystallization in the evolution of the PG. (D) $(La/Yb)_N$ vs Sr/Y plot pinpoints the importance of the partial melting of the subducted oceanic crust in the generation of the PG.

et al., 2005; Darvishi et al., 2015; Tang et al., 2019). The temperature (600–650 °C) and hydrous environment are conformable with a subduction-related setting that can account for the low TiO_2 of the biotites (Fig. 11D). The $FeO_{tot}/(FeO_{tot} + MgO)$ vs MgO(%) suggests that most of the biotites are of crustal origin (Zhou, 1986; Zhang et al., 2015) (SF 7B). This highlights the presence of several components in the generation of the adakitic PG. Clearly, contributions coming from the slab, sediment, crustal material and the upper mantle wedge, in varying degrees, can account for the dominantly subduction-related signature of the PG (Table 3).

5.2. Adakitic Paracale Granodiorite: Components and mechanism of formation

Giese et al. (1986) was the first to recognize that the PG (Paracale Intrusion in their paper) has extremely high Sr content. They arrived at an initial $^{87}Sr/^{86}Sr$ isotopic composition of 0.70352 that led them to consider that the PG was formed by hydrous partial melting of

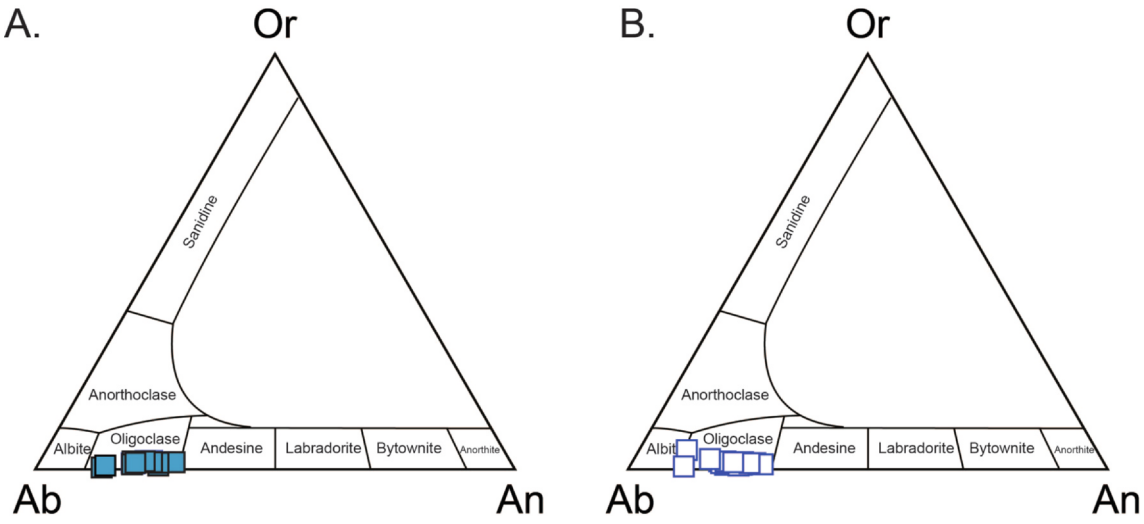

Fig. 10. Or-Ab-An plots of the PG plagioclase cores (A) and rims (B) exhibit a dominant oligoclase composition.

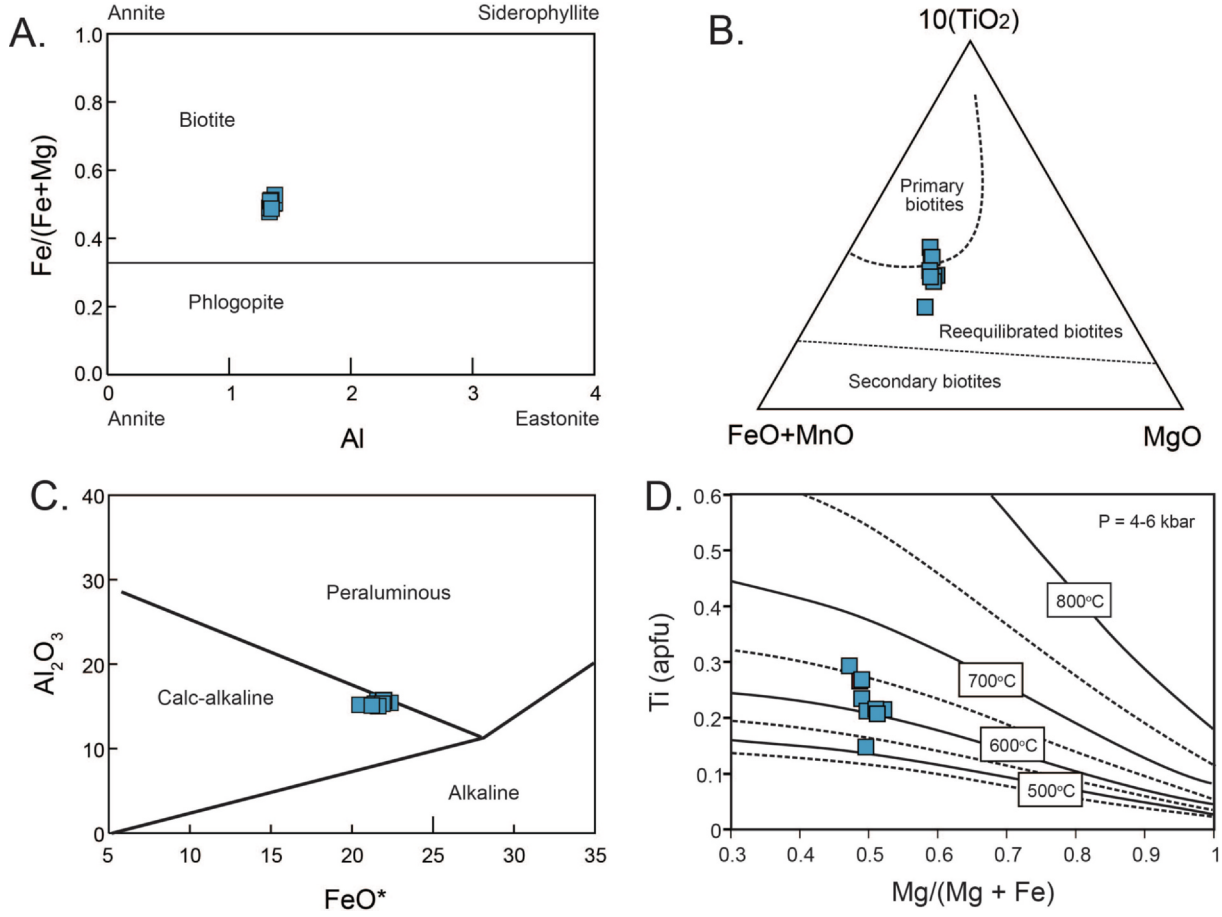

Fig. 11. (A) Al vs Fe/(Fe + MgO) plot indicates that the mica are biotites. (B) TiO_2-FeO + MnO- MgO plot reveals that biotites range from primary to reequilibrated. (C) FeO_{tot} vs Al_2O_3 exhibits the calc-alkaline chemistry of the biotites. (D) A > 600 °C possible crystallization temperature is shown by the Mg/(Mg + Fe) vs Ti diagram. See text for details.

Table 2
Comparison of PG biotites with other granitic complexes. Anorogenic alkaline, peraluminous and calc-alkaline suites are from Abdel-Rahman (1994) and Aydin et al. (2003). Iranian granitoids are from Aydin et al. (2003); Marziyan Granites from Darvishi et al. (2015); and Taihang diorites from Zhang et al. (2015).

Granitic Rocks	FeO_{tot}	MgO	Al_2O_3	FeO_{tot}/MgO
Anorogenic Alkaline Suites	30.60	4.40	11.20	7.04
Peraluminous Suites	22.10	6.30	18.90	3.48
Calc-Alkaline Suites	19.70	11.20	14.90	1.76
Marziyan Granites, NW Iran	0.60–1.8	0.2–1.0	14–18.5	2.6–3
NE Turkey Granitoids	15.8–18.9	12.5–14.2	12.5–13.2	1.1–1.5
Taihang High Mg Diorites (China)	13.8–18.4	11.3–15.8	13.3–14.7	0.9–1.4
Paracale Granodiorite	20.5–22.4	11.1–12.6	15.0–15.7	1.6–1.9

amphibolite associated with MORB. When plotted in the Y versus Sr/Y and Yb_N versus $(La/Yb)_N$, the PG samples exhibit adakitic signature (Fig. 7A,B). The PG samples follow the adakite trend rather than that of the K-enrichment trend typical of calc-alkaline rocks (Kamvong et al., 2014). Partial melting is the dominant process (Fig. 9B) coupled with fluid addition as manifested by the increase in Rb, Ba and Sr (Turner et al., 2012) (Fig. 14A,B). Thick continental crust does not underlie the PG so its role as a possible source of the adakitic magma can be negated. This is supported by the published crustal thickness computations based on gravity data that show a 26–28 km crustal thickness in the Camarines Norte region where the PG is located (Parcutela et al., 2020). The Sr/Y versus Gd/Yb also shows that there is no increase in pressure or thickening of the crust up to the garnet stability field consistent with the absence of a thick continental crust beneath the study area (Fig. 14C). An increase in pressure brought about by thickened crust would have resulted to an increase in Gd/Yb as Yb would be fractionated in the presence of garnet. Thus, the crustal signature indicated by the biotites may have been derived from the overriding oceanic arc. The source region of the PG, for that matter, is possibly characterized by pyroxene or amphibole residues (Fig. 14D). Furthermore, adakites formed through lower crust melting would almost always be in extensional regime accompanied by mafic lavas (e.g. Qian and Hermann, 2013). This is consistent with the low $(La/Yb)_N$ value of the rocks (e.g. Ling et al., 2011; Xue et al., 2017). The PG, as observed in the field, is not associated with any mafic lava. Melting in the eclogite region is supported by the low Yb and as shown by the Y versus Zr/Sm diagram (Fig. 14D). The Nb-Y-Ga^{x3} suggests that the PG is a product of mantle-crust interaction consistent with its K_2O/Na_2O (0.25–0.50) (Eby, 1992; Kamvong et al., 2014) (Fig. 14E,F). The Sr/Y (150–450) and La/Yb (8–40) of the PGs are consistent with slab melts (Sr/Y > 80–100; La/Yb > 30–40) which are much higher than the normal calc-alkaline magmas. The interaction of the melts coming from the slab, sediments, the upper mantle wedge and the base of the crust accounts for the PG geochemistry. This is consistent with the recognition of the involvement and interplay of multiple melt sources of varying geochemistry observed in other arc systems (e.g. Kimura et al., 2005; Durkin et al., 2020). Normal arc magmas generated in the eclogite-amphibolite transition zone in the upper mantle wedge could have interacted with slab and sediment melts (Conder et al., 2002; Kamber et al., 2002; Eiler et al., 2007). The high Mg# (Mg#51–66) of the PG signifies mantle

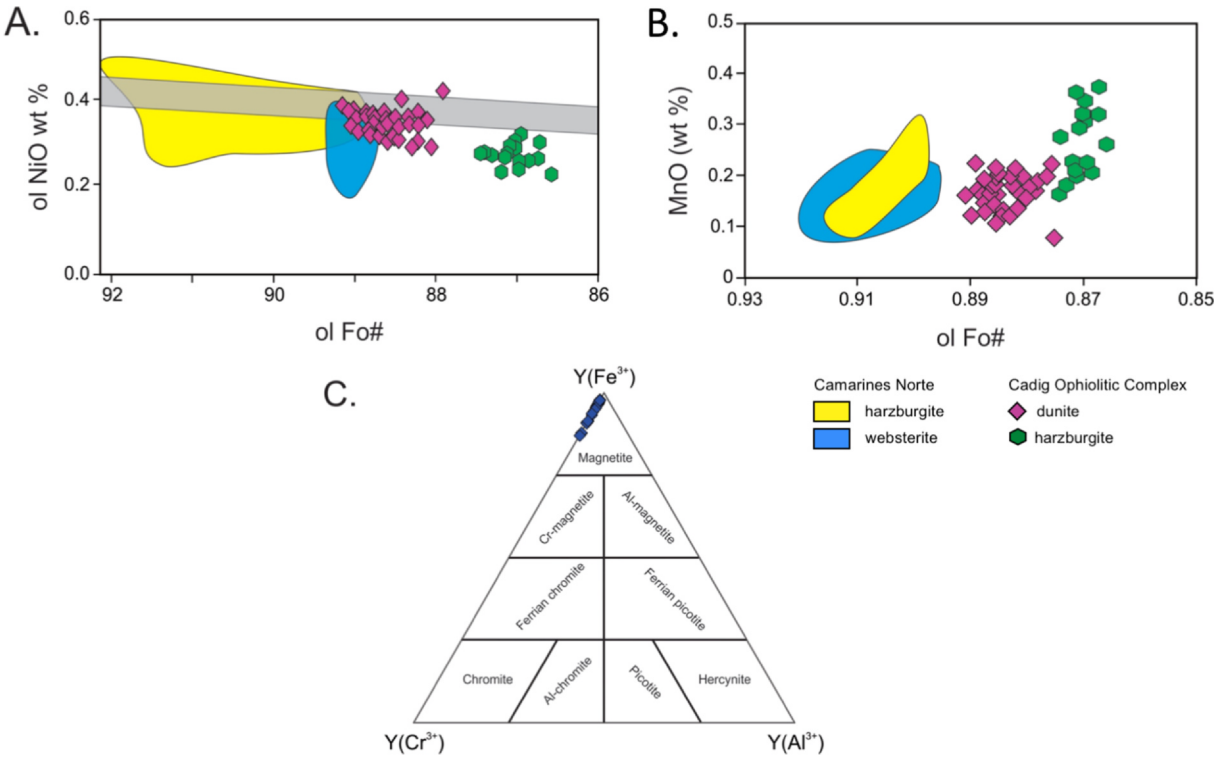

Fig. 12. (A) Fo# vs NiO and (B) Fo# vs MnO plots for the COC dunites and harzburgites reveal their cumulate affinity and are not products of partial melting. The CNOC data for harzburgites and websterites are from Tamayo et al., 1996; Tamayo, 1997. (C) YFe^{3+}-YCr^{3+}-YAl^{3+} plot shows that the COC spinels are all magnetites brought about by serpentinization.

contribution (e.g. Kelemen et al., 2003; Yumul et al., 2003a). The resulting hybrid melt could have ponded at the base of the crust before transiting to the magma chamber and ultimately intruded as adakitic magmas (Fig. 15A). Mantle metasomatism followed by melting, assimilation, storage and homogenization (MASH) with limited fractionation were important processes in generating the PG adakitic rocks similar to what is observed elsewhere (e.g. Maury et al., 1992, 1998; Turner et al., 2012; Ribeiro et al., 2016). The recognition of the PG as having an adakitic character and, at the same time, being a product of MASH with different components (as opposed to that of a pure slab melt) highlights once again that adakite and adakitic rocks must be used as descriptive terms rather than one with a genetic or tectonic setting connotation (Yumul et al., 2000; Castillo, 2012).

5.3. Paracale granodiorite and the birth of the Philippine arc

There are two reported ages (whole rock K-Ar age of 14.9 Ma and $^{40}Ar/^{39}Ar$ biotite age of 18.6 ± 0.3 Ma) for the PG (Wolfe, 1981; Geary et al., 1988). Geary et al. (1988) interpreted the early Miocene age of the igneous body as reflective of the PG's role of being the heat source responsible for the early Miocene regional metamorphism in the area. Our field data, however, do not bear this out. While Mitchell (1988) had opined that the PG represents a tectonic window in structural contact with the ultramafic rocks of the COC, this pluton is observed intruded into the ophiolite. Furthermore, the Upper Eocene to Lower Oligocene Tumbaga Formation contains a lot of ophiolitic and granodiorite clasts which we believe were derived from the PG. These detrital fragments are most evident in the sandstones and conglomerates where detrital mafic and quartz grains, as well as granule- to pebble-sized lithic fragments of peridotite and metamorphosed granodiorite, are observed. This gives a constraint on the age of the PG which is between early Cretaceous (ophiolite age) and late Eocene (Tumbaga Formation).

Interestingly, older intrusive bodies similar to that of PG have been encountered in the Camarines Sur-Albay located south of the study area. The Panganiran Diorite exposed in Pantao Point in Albay yielded a whole-rock K-Ar age of 43.5 Ma (Andal, 2002) (Fig. 1B). The intrusive body has geochemistry similar to that of the PG (Andal, 2002). Another body, the Balatan Andesite, exposed along the coast of Bula, Camarines Sur yielded a whole rock K-Ar age of 68.6 Ma (JICA, 1999) (Fig. 1B). North of the study area, particularly in northeastern Luzon, four magmatic phases have been recognized, the oldest being the Eocene Coastal Batholith (45–39 Ma) (Ringenbach, 1992). Regional correlations would then show that a Cretaceous to early Eocene age for the PG is feasible. If the Eocene age for the PG is correct, then the early to middle Miocene age datings reported by previous workers could represent either a.) reset ages or b.) a younger phase of intrusion within the PG.

The presence of the PG and other intrusive bodies of early Cenozoic age clearly reflects the inception of the Philippine arc in Luzon (Queaño et al., 2020). Although having different approaches, more recent workers (e.g., Queaño et al., 2007; Zahirovic et al., 2014; Wu et al., 2016) have modeled the Philippine arc as occupying sub-equatorial paleolatitudes during the early Cenozoic. These models suggest the Philippine arc as developing either in the East Asia of Wu et al. (2016) or the proto-Philippine Sea Plate (proto-PSP) depicted by Zahirovic et al. (2014) at ~40 Ma. Revision has recently been made in these models, highlighting the presence of a subduction zone (referred to as the proto-East Luzon Trough-Philippine Trench system) separating the Benham Plateau and the Philippine arc during this period (Queaño et al., 2020) (Fig. 15B,C). The spatial distribution of Eocene arc rocks, the presence of Mesozoic ophiolite materials accreted on the eastern coast of the Philippine arc, and the seismic evidence of an old accretionary prism east of Luzon (Lewis and Hayes, 1983) were cited as the principal evidence. Oblique subduction along the proto-East Luzon Trough-Philippine Trench system would also provide the mechanism for the formation of strike-slip faults using the current Philippine tectonic setting as analogue.

While being floored by a Mesozoic ophiolitic suite (in this case, the COC) of proto-PSP origin, David et al. (1997) presented polyphase

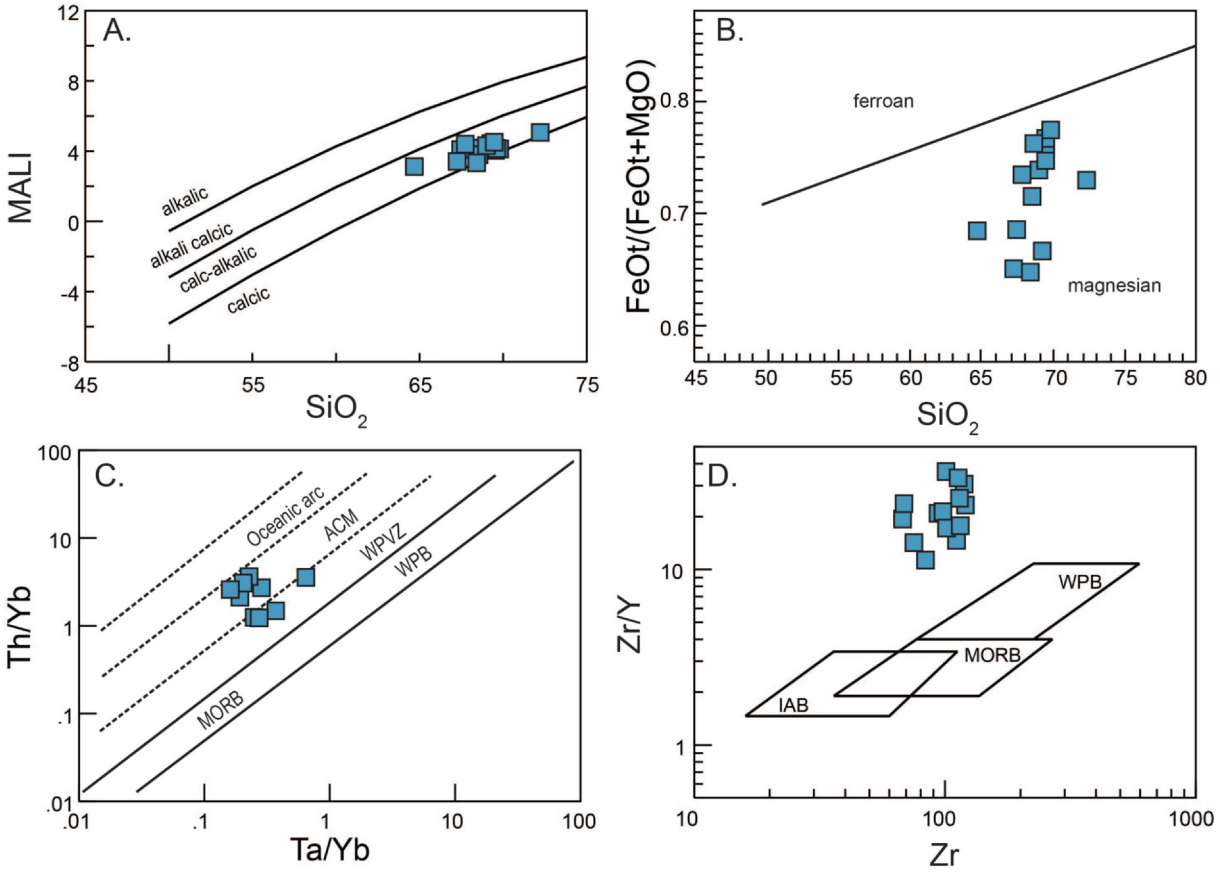

Fig. 13. (A) The SiO_2 vs Modified Alkali-Lime Index (MALI) shows the calc-alkaline affinity of the PG samples. (B) SiO_2 vs $Feo_{tot}/(FeO_{tot} + MgO)$ plot reveals the magnesian character of the PG samples. (C) The Ta/Yb vs Th/Yb plot suggests a strong sediment contribution in the generation of the PG. (D) The Zr vs Zr/Y plot also manifests sediment involvement. Legend: ACM – Active Continental Margin; WPVZ – Within-Plate Volcanic Zone; WPB – Within-Plate Basalt; MORB – Mid-Ocean Ridge Basalt; IAB – Island Arc Basalt.

Table 3
Paracale Granodiorite geochemical characteristics based on published discrimination parameters.

Parameters	Paracale Granodiorite
Shand (1943)	Peraluminous
Ishihara (1977)	Magnetite-type
Pearce et al. (1984)	Volcanic Arc Granite
Maniar and Piccoli (1989)	Orogenic Continental Arc
Defant and Drummond (1990)	Adakitic
Abdel-Rahman (1994) (Biotite)	Calc-alkaline Orogenic Suite
Barbarin (1999)	Arc Continental Granitoid
Bilal and Giret (1999)	Orogenic Granitoid
Chappell and White (2001)	I-type
Frost and Frost (2008)	Magnesian

sinistral movement of the proto-Philippine Fault System as causing the amalgamation of the Mesozoic ophiolite east of the study area and adjacent regions. As reported by previous workers (e.g. David et al., 1996; Tamayo et al., 2004; Yumul, 2007; Dimalanta et al., 2020), these amalgamated ophiolites on the eastern side of the Philippine arc are also of proto-PSP origin. In the eastern part of the Bicol Peninsula, these include the dismembered ophiolites in Calaguas Island (Camarines Norte-Calaguas Island [CNCI]), Lagonoy and Rapu-Rapu island (e.g. Geary and Kay, 1989; Tamayo et al., 1996, 1998; Yumul et al., 2006) (Fig. 1A). All of these ophiolites have been dated as Mesozoic, ranging in age from Jurassic to Late Cretaceous (Geary et al., 1988; David et al., 1997). Almost all of these ophiolite complexes exhibit mid-ocean ridge basalt (MORB) characteristics with muted – island arc tholeiite (IAT) geochemistry. To exemplify, the amphibolite associated with the CNCI has yielded a $^{40}Ar/^{39}Ar$ age date of 99.9 ± 7 Ma which suggests that the CNCI, and by extension, the COC are older than 100 Ma (minimum Early Cretaceous age) (Geary et al., 1988). The geochemistry of the CNCI is generally MORB-like (whole rock TiO_2 = 1.5–2.8 wt%; Al_2O_3/TiO_2 = 4.8–9.6; CaO/TiO_2 = 2.9–6.9; Zr/Y = 1.9–2.9; Olivine Fo# 89.1–92.1; Spinel Cr/(Cr + Al) 33–44; Orthopyroxene Al_2O_3 = 1.58–2.57 wt%) (Geary and Kay, 1989; Tamayo et al., 1996). The olivine of the dunites and, interestingly, the harzburgites of the COC, as plotted in the olivine NiO and MnO versus Fo# indicates a mostly cumulate origin and are not residues of partial melting (Fig. 12A). Although some dunites plot in the olivine mantle array of Takahashi (1986), a lot of the dunites and harzburgites fall outside the array. Most of the samples have undergone intense serpentinization with the orthopyroxene altered to bastites and spinel altered to magnetites (Fig. 12C; SF 6).

In the course of its evolution, a Cretaceous marginal basin within the proto-Philippine Sea Plate received sediments being shed off from nearby landmasses. This will account for the sediment signatures (high Th, Zr/Y) that are recognized in the PG. As spreading ensued within this marginal basin to mark the inception of the Philippine Sea Plate, subduction was also initiated on the eastern side of the Philippine arc (based on the present geography). Continuous subduction beneath the overriding plate, of which the COC is part of, resulted in the development of an arc, being the adakitic PG suite (Fig. 15B,C). With this, the PG represents the earliest magmatic, albeit adakitic, product of early Cenozoic (possibly extending back to the Late Mesozoic) subduction of the proto-Philippine Sea Plate.

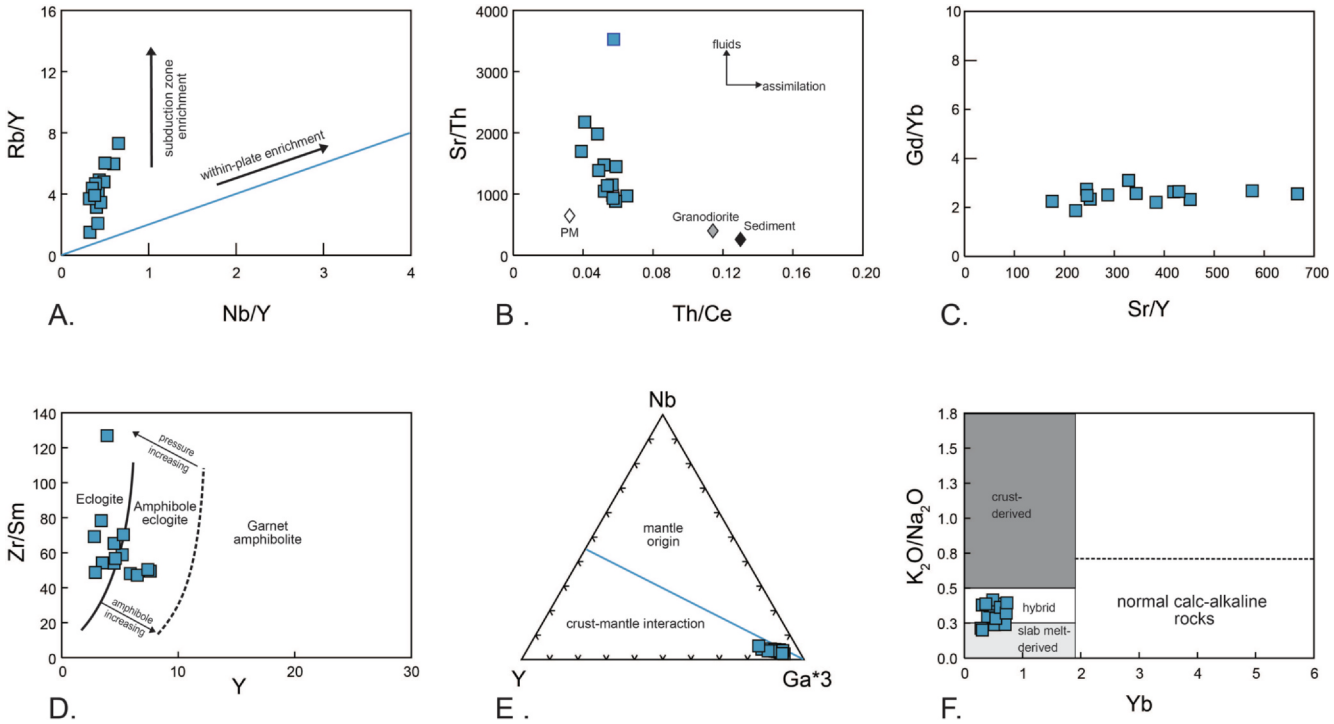

Fig. 14. (A) Nb/Y vs Rb/Y (after Termel et al., 1998) shows the importance of subduction contribution in PG generation. (B) Th/Ce vs Sr/Th plot is consistent with fluid addition. (C) Sr/Y vs Gd/Yb (after Mori et al., 2007) indicates no thickening of the crust and the absence of garnet in the source region. (D) Y vs Zr/Sm suggests melting occurred in the eclogite-amphibolite zone. (E) Nb-Y-Ga*3 indicates that the PG are products of crust-mantle interaction. (F) The Yb vs K_2O/Na_2O plot is consistent with the PG as a hybrid magma made up of slab and crustal components. See text for details. Legend: PM – Primordial Mantle.

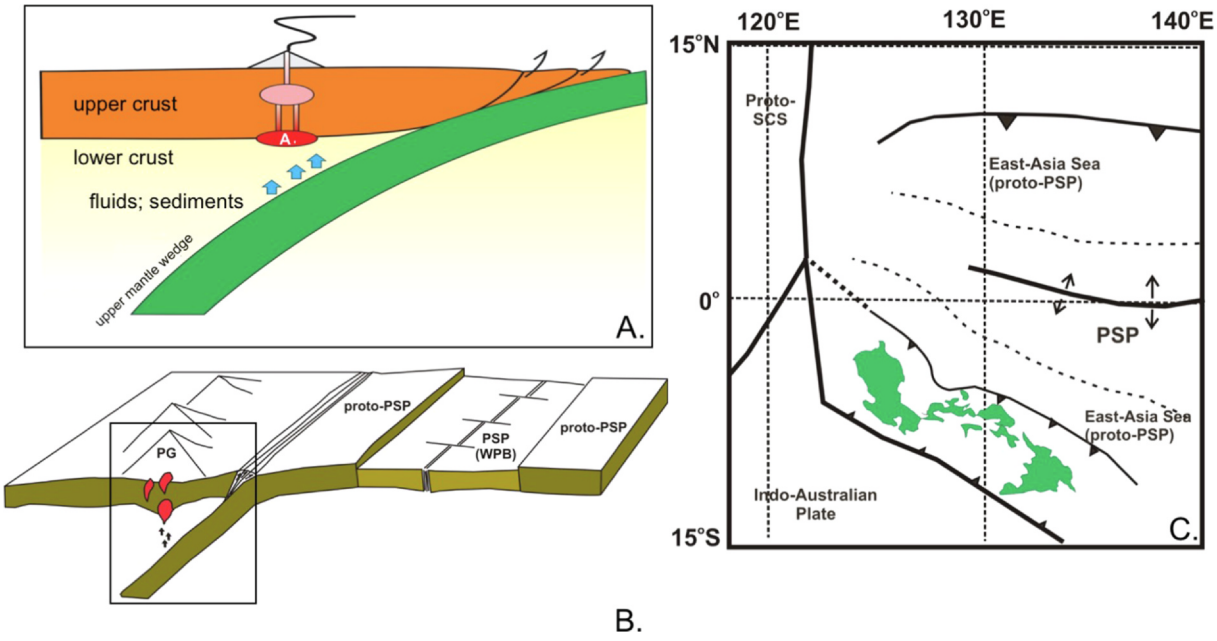

Fig. 15. (A) Cartoon model showing the different components responsible for the formation of the PG. (B) Schematic model and (C) Palinspastic map showing the generation of the PG. Legend: A – Mixed, adakitic melts; PSP – Philippine Sea Plate; WPB – West Philippine Basin; SCS – South China Sea.

6. Conclusions

The PG exhibits calc-alkaline characteristics and has trondhjemitic–adakitic affinity. Quartz and plagioclase with minor biotite, apatite, titanate and oxide minerals are the fractionating phases. Whole rock and biotite mineral chemistry are consistent with a subduction-related setting. A hydrous environment with a temperature of ~600 °C characterizes the melt that formed the PG. The PG manifests adakitic geochemical characteristics. Several components ranging from slab melt, upper mantle material, sediments and crust materials contributed into the generation of the hybrid slab-crustal adakitic PG melt. Slab and sediment melting that interacted with the mantle and crust, through melting, assimilation, storage and homogenization (MASH) could explain the adakitic character of the PG. The tectonic setting from where this adakitic rock suite formed was in an orogenic subduction complex. The PG, which is intruded into an ultramafic-mafic complex, the Cadig

Ophiolitic Complex, represents the earliest adakitic product related to the late Mesozoic to early Paleogene proto-Philippine Sea Plate subduction event.

Declaration of Competing Interest

The authors declare that they have no known competing financial interests or personal relationships that could have appeared to influence the work reported in this paper.

Acknowledgements

The assistance extended by the members of the Rushurgent Working Group during the field surveys, in the laboratory analyses and discussion of results is acknowledged. Dr. Juan Miguel Guotana and Efren Gadot did the microprobe analyses. Engr. Modesto B. Bermudez of the Paracale Gold Ltd. and Dr. Walter W. Brown of Apex Mining Co., Inc. are thanked for the encouragement, support and guidance extended to the group. The extensive work of Rodolfo A. Tamayo Jr. (RIP) on the Bicol ophiolites has been a major part of this study. The UP-NIGS EPMA was procured under a Philippine Department of Science and Technology research grant to UP Diliman.

Appendix A. Supplementary material

Supplementary data to this article can be found online at https://doi.org/10.1016/j.jaesx.2020.100035.

References

Abdel-Rahman, A.M., 1994. Nature of biotites from alkaline, calcalkaline and peraluminous magmas. J. Petrol. 35, 525–541.
Andal, E.S., 2002. Geological and geochemical characterization of the Plio-Pleistocene to Recent volcanic rocks of the Southeastern Luzon volcanic arc chain: Implications to arc evolution. M.Sc. thesis, University of the Philippines, 154 pp.
Andal, E.S., Yumul Jr., G.P., Listanco, E.L., Tamayo Jr., R.A., Dimalanta, C.B., Ishii, T., 2005. Characterization of the Pleistocene volcanic chain of the Bicol Arc, Philippines: implications for geohazard assessment. Terrestrial Atmos. Oceanic Sci. 16, 865–883.
Arai, S., Tamura, A., Miura, M., Seike, K., 2018. Abyssal peridotite as a component of forearc mantle: Inference from a new mantle xenolith suite of Bankawa in the Southwest Japan arc. Art. 540. Minerals 8. https://doi.org/10.3390/min8110540.
Aydin, F., Karsli, O., Sadiklar, M.B., 2003. Mineralogy and chemistry of biotites from Eastern Pontide Granitoid Rocks, NE-Turkey: Some petrological implications for granitoid magmas. Chemie der Erde Geochemistry 63, 163–182.
Barbarin, B., 1999. A review of the relationships between granitoid types, their origins and their geodynamic environments. Lithos 46, 605–626.
Barnes, S.J., Roeder, P.L., 2001. The range of spinel compositions in terrestrial mafic and ultramafic rocks. J. Petrol. 12, 2279–2302.
Barrier, E., Huchon, P., Aurelio, M., 1991. Philippine Fault: a key for the Philippine kinematics. Geology 19, 32–35.
Bellon, H., Yumul Jr., G.P., 2001. Miocene to Quaternary adakites and related rocks in Western Philippine arc sequences. Comptes Rendus de l'Academie des Sciences 333, 343–350.
Bilal, E., Giret, A., 1999. The aluminum saturation index and the MgO/TiO_2 ratio: Two parameters influenced by PH_2O and their use to discriminate magma series. Revista Brasileira de Geosciencias 29, 55–58.
Bryner, L., 1969. Ore deposits of the Philippines - an introduction to their geology. Econ. Geol. 64, 644–666.
Castillo, P.R., 2012. Adakite petrogenesis. Lithos 134, 304–316. https://doi.org/10.1016/j.lithos.2011.09.013.
Castillo, P.R., Janey, P.E., Solidum, R.U., 1999. Petrology and geochemistry of Camiguin Island, Southern Philippines: insight to the source of adakites and other lavas in a complex arc setting. Contrib. Miner. Petrol. 134, 33–51.
Castillo, P.R., Newhall, C.G., 2004. Geochemical constraints on possible subduction components in lavas of Mayon and Taal Volcanoes, Southern Luzon, Philippines. J. Petrol. 45, 1089–1108.
Chappell, B.W., White, A.J.R., 1974. Two contrasting granite types. Pac. Geol. 8, 173–174.
Chappell, B.W., White, J.R., 2001. Two contrasting granite types: 25 years later. Aust. J. Earth Sci. 48, 489–499.
Comsti, M.E.C., de Jesus, C.V., Marcelo, M.T.R., 1985. Temperatures of gold-quartz vein formation at Olecram Mining Corporation, Jose Panganiban, Camarines Norte as indicated by fluid inclusions. Philippine Geol. 39, 35–47.
Conder, J.A., Wiens, D.A., Morris, J., 2002. On the decompression melting structure at volcanic arcs and back-arc spreading centers. Geophys. Res. Lett. 29. https://doi.org/10.1029/2002GL015390.
Cox, K.G., Bell, J.D., Pankhurst, R.J., 1979. The Interpretation of Igneous Rocks, George, Allen and Unwin, Ltd., London, 450 pp.
Cox, G.M., Foden, J., Collins, A.S., 2018. Late Neoproterozoic adakitic magmatism of the eastern Arabian Nubian Shield. Geosci. Front. https://doi.org/10.1016/j.gsf2017.12.006.
Darvishi, E., Khalili, M., Beavers, R., Sayari, M., 2015. Petrology and mineral chemistry of paraluminous Marziyan granites, Sanandaj-Sirjan metamorphic belt (NW Iran). Geol. Carpath. 66, 361–374.
David Jr., S.D., Stephan, J.F., Delteil, J., Muller, C., Bellon, H., Sajona, F.G., 1996. Geology, geochemistry, geochronology and structures of the ophiolites in Southeastern Luzon, Philippines. J. Geol. Soc. Philippines 51, 115–129.
David Jr., S.D., Stephan, J.F., Delteil, J., Muller, C., Butterlin, J., Bellon, H., Billedo, E., 1997. Geologic and tectonic history of southeastern Luzon, Philippines. J. Asian Earth Sci. 15, 435–452.
Deer, W.A., Howie, R.A., Zussman, J., 1996. An Introduction to the Rock-forming Minerals. John Wiley and Sons, New York, pp. 528.
Defant, M.J., Drummond, M.S., 1990. Derivation of some modern arc magmas by melting of young subducted lithosphere. Nature 347, 662–665.
Defant, M.J., Xu, J.F., Kepezhinskas, P., Wang, Q., Zhang, Q., Xiao, L., 2002. Adakites: some variations on a theme. Acta Petrol. Sin. 18, 129–142.
Deng, J., Yang, X., Qi, H., Zhang, Z.-F., Mastoi, A.S., Sun, W., 2017. Early Cretaceous high-Mg adakites associated with Cu-Au mineralization in the Cebu island, Central Philippines: implication for partial melting of the paleo-Pacific Plate. Ore Geol. Rev. http://dx.doi.org/10.1016/j.oregeorev2017.05.006.
Deng, J., Yang, X., Qi, H., Zhang, Z.-F., Mastoi, A.S., Berador, A.E.G., Sun, W., 2019. Early Cretaceous adakite from the Atlas porphyry Cu-Au deposit in Cebu Island, Central Philippines: partial melting of subducted oceanic crust. Ore Geol. Rev. 110. https://doi.org/10.1016/j.oregeorev.2019.102937.
Dimalanta, C.B., Faustino-Eslava, D., Gabo-Ratio, J.A.S., Marquez, E.J., Padrones, J.T., Payot, B.D., Queaño, K.L., Ramos, N.T., Yumul Jr., G.P., 2020. Characterization of the proto-Philippine Sea Plate: evidence from the emplaced oceanic lithospheric fragments along eastern Philippines. Geosci. Front. 11, 3–12. https://doi.org/10.1016/j.gsf.2019.01.005.
Durkin, K., Castillo, P.R., Straub, S.M., Abe, N., Tamura, Y., Yan, Q., 2020. An origin of the along-arc compositional variation in the Izu-Bonin arc system. Geosci. Front. 11, 1621–1634.
Eiler, J.M., Schiano, P., Valley, J.W., Kita, N.T., Stolper, E.M., 2007. Oxygen-isotope and trace element constraints on the origins of silica-rich melts in the subarc mantle. Geochem. Geophys. Geosyst. 8, Q09012. https://doi.org/10.1029/2006GC001503.
Eby, G.N., 1992. Chemical subdivision of the A-type granitoids: Petrogenetic and tectonic implications. Geology 20, 641–644.
Encarnacion, J., 2004. Multiple ophiolite generation preserved in the northern Philippines and the growth of an island arc complex. Tectonophysics 392, 103–130.
Foster, M.D., 1960. Interpretation of the composition of trioctahedral micas. Geological Survey Professional Paper 354-B, 43 pp.
Frost, J.E., 1965. Controls of ore deposition for the Larap mineral deposits, Camarines Norte, Philippines. Ph.D. dissertation. Stanford University, 173 pp.
Frost, B.R., Barnes, C.G., Collins, W.J., Arculus, R.J., Ellis, D.J., Frost, C.D., 2001. A geochemical classification for granitic rocks. J. Petrol. 42, 2033–2048.
Frost, B.R., Frost, C.D., 2008. A geochemical classification for feldspathic igneous rocks. J. Petrol. 49, 1955–1969.
Gargiulo, M.F., Bjerg, E.A., Mogessie, A., 2013. Spinel group minerals in metamorphosed ultramafic rocks from Rio de las Tunas belt, Central Andes, Argentina. Geol. Acta 11, 133–148.
Geary, E., Kay, R., 1989. Identification of an early Cretaceous ophiolite in the Camarines Norte-Calaguas islands basement complex, eastern Luzon, Philippines. Tectonophysics 168, 109–126.
Geary, E.E., Mark Harrison, T., Heizler, M., 1988. Diverse ages and origins of basement complexes, Luzon, Philippines. Geology 16, 341–344.
Gebco Compilation Group, 2019. GEBCO 2019 Grid, doi:10.5285/836f0f16a-33be-6ddc-e053-6c86abc0788e.
Giese, U., Knittel, U., Kramm, U., 1986. The Paracale Intrusion: geologic setting and petrogenesis of a trondhjemite intrusion in the Philippine Island Arc. J. SE Asian Earth Sci. 1, 235–245.
Haggerty, S.E., 1991. Oxide mineralogy of the upper mantle. Spinel mineral group. In: Lindsley, D.H. (Ed.), Reviews in Mineralogy, Oxide minerals: Petrologic and magnetic significance. Mineralogical Society of America 25, 355-416.
Henry, D.J., Guidotti, C., Thomson, J.A., 2005. The Ti-saturation surface for low-to-medium pressure metapelitic biotites: implications for geothermometry and Ti-substitution mechanisms. Am. Mineral. 90, 316–328.
Hernandez-Uribe, D., Hernadez-Montenegro, J.D., Cone, K.A., Palin, R.M., 2020. Oceanic slab-top melting during subduction: implications for trace-element recycling and adakite petrogenesis. Geology 48, 216–220.
Hildebrand, R.S., Whalen, J.B., 2014. Arc and slab-failure magmatism in Cordilleran batholiths II – The Cretaceous Peninsular Ranges Batholith of Southern and Baja California. Geoscience Canada 41, http://dx.doi.org/10.12789/geocanj.2014.41.059.
Hu, Y.-B., Liu, J.-Q., Ling, M.-X., Liu, Y., Ding, X., Liu, D.-Y., Sun, W.-D., 2017. Constraints on the origin of adakites and porphyry Cu-Mo mineralization in Chongjiang, Southern Gangdese, the Tibetan Plateau. Lithos 292–293, 424–436.
Irvine, T.N., Baragar, W.R.A., 1971. A guide to the chemical classification of the common volcanic rocks. Can. J. Earth Sci. 8, 523–548.
Ishihara, S., 1977. The magnetite-series and ilmenite-series granitic rocks. Mining Geol. 27, 293–305.
Japan International Cooperation Agency (JICA), 1999. Report on the Regional Survey for Mineral Resources in the Bicol Arc, Tokyo, Japan.

Jarvis, A., Reuter, H.I., Nelson, A., Guevara, E., 2008. Hole-filled SRTM for the globe Version 4. International Centre for Tropical Agriculture (CIAT). Accessed from https://srtm.csi.cgiar.org on July 15, 2020.
Jego, S., Maury, R.C., Polve, M., Yumul Jr., G.P., Bellon, H., Tamayo Jr., R.A., Cotten, J., 2005. Geochemistry of adakites from the Philippines: constraints on their origins. Resour. Geol. 55, 161–185.
Ji, D., Liu, H., Li, Y., 2019. Large-scale early Cretaceous lower-crust melting derived adakitic rocks in NE China: implications for convergent bidirectional subduction and slab rollback. Int. Geol. Rev. https://doi.org/10.1080/00206814.2019.1697968.
Kamber, B.S., Ewart, A., Collerson, K.D., Bruce, M.C., McDonald, G.D., 2002. Fluid-mobile trace element constraints on the role of slab melting and implications for Archaean crustal growth models. Contrib. Miner. Petrol. 144, 38–56.
Kamei, A., 2004. An adakitic pluton on Kyushu Island, southwest Japan arc. J. Asian Earth Sci. 24, 43–58.
Kamei, A., Miyake, Y., Owada, M., Kimura, J.-I., 2009. A pseudo-adakite derived from partial melting of tonalitic to granodioritic crust, Kyushu, southwest Japan arc. Lithos 112, 615–625.
Kamvong, T., Zaw, K., Meffre, S., Maas, R., Stein, H., Lai, C.-K., 2014. Adakites in the Truong Son and Loei fold belts, Thailand and Laos: genesis and implications for geodynamics and metallogeny. Gondwana Res. 26, 165–184.
Karig, D.E., 1983. Accreted terranes in the northern part of the Philippine archipelago. Tectonics 2, 211–236.
Karimpour, M.H., Stern, C.R., Mouradi, M., 2011. Chemical composition of biotite as a guide to petrogenesis of granitic rocks from Maherabad, Dehnow, Gheshlagh, Khajehmourad and Najmabad, Iran. Iranian J. Crystall. Mineral. 18, 89–100.
Kay, S.M., Mpodozis, C., 2001. Central Andean ore deposits linked to evolving shallow subduction systems and thickening crust. GSA Today 11, 4–9.
Kelemen, P.B., Yogodzinski, G.M., Scholl, D.W., Eiler, J.M., 2003. Along-strike variation in the Aleutian island arc: genesis of high Mg# andesite and implications for continental crust. Geophys. Monograph 138, 223–276.
Kimura, J.-I., Stern, R.J., Yoshida, T., 2005. Reinitiation of subduction and magmatic responses in SW Japan during Neogene time. Geol. Soc. Am. Bull. 117, 969–986.
Le Bas, M.J., Lemaitre, R.W., Streckeisen, A., Zanettin, B., 1986. A chemical classification of volcanic rocks based on the total alkali-silica diagram. J. Petrol. 27, 745–750.
Lewis, S.D., Hayes, D.E., 1983. The tectonics of northward propagating Subduction along eastern Luzon, Philippine islands. In: Hayes, D.E. (Ed.), The Tectonic and Geologic Evolution of South East Asian Seas and Islands, Part 2. Geophysical Monograph Series 27, AGU, Washington, D.C., pp. 57–78.
Li, Y.-B., Kimura, J.-I., Machida, S., Ishii, T., Ishiwatari, A., Maruyama, S., Qiu, H.-N., Ishikawa, T., Kato, Y., Haraguchi, S., Takahata, N., Hirahara, Y., Miyazaki, T., 2013. High-Mg adakite and low-Ca boninite from a Bonin fore-arc seamount: implications for the reaction between slab melts and depleted mantle. J. Petrol. 54 (6), 1149–1175.
Lin, P.-N., Stern, R.-J., Bloomer, S.H., 1989. Shoshonitic volcanism in the northern Mariana arc. 2. Large-ion lithophile and rare earth element abundances: evidence for the source of incompatible element enrichments in intraoceanic arcs. J. Geophys. Res. 94, 4497–4514.
Ling, M.-X., Wang, F.-Y., Ding, X., Zhou, J.-B., Sun, W., 2011. Different origins of adakites from the Dabie Mountains and the Lower Yangtze River Belt, eastern China: geochemical constraints. Int. Geol. Rev. 53, 727–740.
Luhr, J.F., Carmichael, I.S.E., Verekamp, J.C., 1984. The 1982 eruptions of El Chichon volcano, Chiapas, Mexico: mineralogy and petrology of the anhydrite-bearing pumices. J. Volcanol. Geoth. Res. 23, 69–108.
Macpherson, C.G., Dreher, S.T., Thirlwall, M.F., 2006. Adakites without slab melting: high pressure differentiation of island arc magma, Mindanao, the Philippines. Earth Planet. Sci. Lett. 243, 581–593.
Maniar, P.D., Piccoli, P.M., 1989. Tectonic discrimination of granitoids. Geol. Soc. Am. Bull. 101, 635–643.
Martin, H., 1999. Adakitic magmas: modern analogues of Archaean granitoids. Lithos 46, 411–429.
Martin, H., Smithies, R.H., Rapp, R., Moyen, J.-F., Champion, D., 2005. An overview of adakite, tonalite-trondhjemite-granodiorite (TTG), and sanukitoid relationships and some implications for crustal evolution. Lithos 79, 1–24.
Maury, R.C., Defant, M.J., Bellon, H., Jacques, D., Joron, J.-L., McDermott, F., Vidal, P., 1998. Temporal geochemical trends in northern Luzon arc lavas (Philippines): implications on metasomatic processes in the island arc mantle. Bull. Geol. Soc. France 169, 69–80.
Maury, R.C., Defant, M.J., Joron, J.L., 1992. Metasomatism of the sub-arc mantle inferred from trace elements in Philippine xenoliths. Nature 360, 661–663.
Maury, R.C., Sajona, F.C., Pubellier, M., Bellon, H., Defant, M.J., 1996. Fusion de la croute oceanique dans les zones de subduction/collision recentes: l'exemple de Mindanao (Philippines). Bull. Soc. Geol. Fr. 167, 579–595.
McCabe, R., Almasco, J., Yumul, G.P.Jr., 1985. Terranes in the Central Philippines. In: Howell, D. (Ed.), Tectonostratigraphic Terranes of the Circum-Pacific Region, Earth Series 1, 421–35.
Metal Mining Agency of Japan – Japan International Cooperation Agency (MMAJ-JICA), 1994. Basic Design Study Report on the Rural Environmental Sanitation Project in the Republic of the Philippines (Phase III), 92 pp.
Metal Mining Agency of Japan – Japan International Cooperation Agency (MMAJ-JICA), 1998. Report on the Mineral Exploration in the Bicol Area. The Republic of the Philippines (Phase 1), 79pp.
Mines and Geosciences Bureau (MGB), 2010. Geology of the Philippines, 2nd edition, Quezon City, Philippines, 532 pp.
Miranda, F.E., Caleon, P.C., 1979. Geology and mineral resources of Camarines Norte and Part of Quezon Province. Bureau Mines Report Invest. 94, 101 pp.
Mitchell, A.H.G., 1988. Discussion on the Paracale Intrusion in the Philippines. J. SE Asian Earth Sci. 2, 241–296.
Mitchell, A.H.G., Balce, G.R., 1990. Geological features of some epithermal gold systems, Philippines. J. Geochem. Explor. 35, 241–296.
Mitchell, A.H.G., Fernandez, F., de la Cruz, A.P., 1986. Cenozoic evolution of the Philippine Archipelago. J. SE Asian Earth Sci. 1, 3–22.
Moradi, R., Boomeri, M., Bagheri, S., Nakashima, K., 2016. Mineral chemistry of igneous rocks in the Lar Cu-Mo prospect, southeastern part of Iran: Implications for P, T, and fO_2. Turk. J. Earth Sci. 25, 418–433.
Mori, L., Gómez-Tuena, A., Cai, Y., Goldstein, S.L., 2007. Effects of prolonged flat subduction on the Miocene magmatic record of the central Trans-Mexican Volcanic Belt. Chem. Geol. 244, 452–473.
Moyen, J.-F., 2009. High Sr/Y and La/Yb ratios: the meaning of the "adakitic signature". Lithos 112, 556–574.
Nachit, H., Ibhi, A., Abia, E.-H., Ohoud, M.-B., 2005. Discrimination between primary magmatic biotites, reequilibrated biotites and neoformed biotites. C. R. Geosci. 337, 1415–1420.
Nakamura, H., Iwamori, H., 2013. Generation of adakites in a cold subduction zone due to double subducting plates. Contrib. Miner. Petrol. 165, 1107–1134.
Ozawa, A., Tagami, T., Listanco, E.L., Arpa, C.B., Sudo, M., 2004. Initiation and propagation of subduction along the Philippine Trench: Evidence from the temporal and spatial distribution of volcanoes. J. Asian Earth Sci. 23, 105–111.
Parcutela, N.E., Dimalanta, C.B., Armada, L.T., Yumul Jr., G.P., 2020. PHILCRUST3.0: New constrainsts in crustal growth rate computations for the Philippine arc. J. Asian Earth Sci. X. https://doi.org/10.1016/j.jaesx.2020.100032.
Pearce, J.A., 1982. Trace element characteristics of lavas from destructive plate boundaries. In: Thorpe, R.S. (Ed.), Andesites: Orogenic Andesites and Related Rocks. John Wiley and Sons, Chichester, England, pp. 528–548.
Pearce, J.A., Harris, B.W., Tindle, A.G., 1984. Trace element discrimination diagrams for the tectonic interpretation of granitic rocks. J. Petrol. 25, 956–983.
Pearce, J.A., Norry, M.J., 1979. Petrogenetic implications of Ti, Zr, Y, and Nb variations in volcanic rocks. Contrib. Miner. Petrol. 69, 33–47.
Peccerillo, A., Taylor, S.R., 1976. Geochemistry of Eocene calc-alkaline volcanic rocks from the Kastamonu Area, Northern Turkey. Contrib. Miner. Petrol. 58, 63–81.
Polve, M., Maury, R.C., Jego, S., Bellon, H., Margoum, A., Yumul Jr., G.P., Payot, B.D., Tamayo Jr., R.A., Cotten, J., 2007. Temporal geochemical evolution of Neogene magmatism in the Baguio gold–copper Mining District (Northern Luzon, Philippines). Resour. Geol. 57, 197–218.
Qian, Q., Hermann, J., 2013. Partial melting of lower crust at 10–15 kbar: constraints on adakite and TTG formation. Contrib. Miner. Petrol. 165, 1195–1224.
Queaño, K.L., Ali, J.R., Milsom, J., Aitchison, J.C., Pubellier, M., 2007. North Luzon and the Philippine Sea Plate motion model: insights following paleomagnetic, structural, and age-dating investigations. J. Geophys. Res. Solid Earth 112, B5.
Queaño, K.L., Ali, J.R., Pubellier, M., Yumul Jr., G.P., Dimalanta, C.B., 2009. Reconstructing the Mesozoic – early Cenozoic evolution of northern Philippines: clues from palaeomagnetic studies on the ophiolitic basement of the Central Cordillera. Geophys. J. Int. 178, 1317–1326.
Queaño, K.L., Yumul Jr., G.P., Marquez, E.J., Gabo-Ratio, J.A., Payot, B.D., Dimalanta, C.B., 2020. Consumed tectonic plates in Southeast Asia: markers from the Mesozoic to early Cenozoic stratigraphic units in the northern and central Philippines. J. Asian Earth Sci. X. https://doi.org/10.1016/j.jaesx.2020.100033.
Quebral, R., Pubellier, M., Rangin, C., 1996. The onset of movement on the Philippine Fault in eastern Mindanao: a transition from a collision to strike-slip environment. Tectonics 15, 713–726.
Rangin, C., 1991. The Philippine mobile belt: a complex plate boundary. J. SE Asian Earth Sci. 6, 209–220.
Ribeiro, J.M., Maury, R.C., Grégoire, M., 2016. Are adakites slab melts or high-pressure fractionated mantle melts? J. Petrol. 57, 839–862.
Richards, J.P., 2011. High Sr/Y arc magmas and porphyry Cu ± Au deposits: just add water. Econ. Geol. 106, 1075–1081.
Richards, J.P., Kerrich, R., 2007. Adakite-like rocks: their diverse origin and questionable role in metallogenesis. Econ. Geol. 102, 537–576.
Rieder, M., Cavazzini, G., D'Yakonov, Y.S., Frank-Kamenetskii, V.A., Gottardi, G., Guoggenheim, S., Koval, P.V., Muller, G., Neiva, A.M.R., Radoslovich, E.W., et al., 1998. Nomenclature of the micas. Can. Mineral. 36, 905–912.
Ringenbach, J.C., 1992. La faille Philippine et les chaines en decrochement associees (centre-nord Luzon): Evolution cenozoique et cinematique des deformations quaternaires. Ph.D. Thesis. Universite de Nice, 316 pp.
Sajona, F.G., Bellon, H., Maury, R.C., Pubellier, M., Quebral, R.D., Cotten, J., Bayon, F., Pagado, E., Pamatian, P., 1997. Tertiary and Quaternary magmatism in Mindanao (Philippines): geochronology, geochemistry and tectonic setting. J. Asian Earth Sci. 15, 121–153.
Sajona, F.G., Maury, R.C., 1998. Association of adakites with gold and copper mineralization in the Philippines. Comptes Rendus de l'Academie des Sciences 326, 27–34.
Sajona, F.G., Maury, R.C., Bellon, H., Cotten, J., Defant, M.J., Pubellier, M., Rangin, C., 1993. Initiation of subduction and the generation of slab melts in western and eastern Mindanao, Philippines. Geology 27, 1007–1010.
Sajona, F.G., Maury, R.C., Prouteau, G., Cotten, J., Schiano, P., Bellon, H., Fontaine, L., 2000. Slab melt as metasomatic agent in island arc magma mantle sources, Negros and Batan (Philippines). Isl. Arc 9, 472–486.
Shand, S.J., 1943. Eruptive rocks. Their Genesis, Composition, Classification, and Their Relations to Ore-Deposits. Wiley, New York, pp. 1–444.
Sherlock, R.L., Barrett, T.J., Lewis, P.D., 2003. Geological setting of the Rapu Rapu gold-rich volcanogenic massive sulfide deposits, Albay Province, Philippines. Miner. Deposita 38, 813–830.
Sun, S., McDonough, W.F., 1989. Chemical and isotopic systematics of oceanic basalts: implications for mantle composition and processes. In: In: Saunders, A.D., Norry, M.J.

(Eds.), Magmatism in the Ocean Basins 42. Geological Society of London Special Publication, pp. 313–345.
Takahashi, E., 1986. Origin of basaltic magmas: Implications from peridotite melting experiments and olivine fractionation model. Bull. Volcanol. Soc. Japan 30, S17–S40.
Tamayo Jr., R.A., 1997. Petrological and geochemical characterization of the Camarines Norte Ophiolite Complex. M.Sc. thesis. University of the Philippines.
Tamayo Jr., R.A., Maury, R.C., Yumul Jr., G.P., Polve, M., Cotten, J., Dimalanta, C.B., Olaguera, F.O., 2004. Subduction-related magmatic imprint of most Philippine ophiolites: implications on the early geodynamic evolution of the Philippine archipelago. Bull. Geol. Soc. France 175, 443–460.
Tamayo Jr., R.A., Yumul Jr., G.P., Jumawan, F., 1996. Geology and geochemistry of the mafic rock series of the Camarines Norte Ophiolite Complex. J. Geol. Soc. Philippines 3, 131–152.
Tamayo Jr., R.A., Yumul Jr., G.P., Santos, R.A., Jumawan, F., Rodolfo, K.S., 1998. Petrology and mineral chemistry of a back-arc upper mantle suite: example from the Camarines Norte Ophiolite Complex, south Luzon. J. Geol. Soc. Philippines 53, 1–23.
Tang, M., Lee, C.-T.A., Chen, K., Erdman, M., Costin, G., Jiang, H., 2019. Nb/Ta systematics in arc magma differentiation and the role of arclogites in continent formation. Nat. Commun. https://doi.org/10.1038/s41467-018-08198-3.
Temizel, I., Arslan, M., Yucel, C., Yazar, E.A., Kaygusuz, A., Aslan, Z., 2019. Eocene tonalite-granodiorite from the Havza (Samsun) area, northern Turkey: adakite-like melts of lithospheric mantle and crust generated in a post-collisional setting. Int. Geol. Rev. https://doi.org/10.1080/00206814.2019.1625077.
Termel, A., Gtlndogdu, M.N., Gourgaud, A., 1998. Petrological and geochemical characteristics of Cenozoic high K calc-alkaline volcanism in Konya, Central Anatolia, Turkey. J. Volcanol. Geoth. Res. 85, 327–354.
Thorkelson, D.J., Breitsprecher, K., 2005. Partial melting of slab window margins: genesis of adakitic and non-adakitic magmas. Lithos 79, 25–41.
Torkian, A., Furman, T., Salehi, N., Veloski, K., 2019. Petrogenesis of adakites from the Sheyda volcano, NW Iran. J. Afr. Earth Sc. 150, 194–204.
Turner, S., Caulfield, J., Turner, M., van Kekn, P., Maury, R., Sandiford, M., Proteau, G., 2012. Recent contribution of sediments and fluids to the mantle's volatile budget. Nat. Geosci. 5, 50–54.
Whalen, J.B., Currie, K.L., Chappell, B.W., 1987. A-type granites: geochemical characteristics, discrimination and petrogenesis. Contrib. Miner. Petrol. 95, 407–419.
Winchester, J.A., Floyd, P.A., 1977. Geochemical discrimination of different magma series and their differentiation products using immobile elements. Chem. Geol. 20, 325–343.
Wolfe, J.A., 1981. Philippine geochronology. J. Geol. Soc. Philippines 35, 1–30.
Wones, D.R., 1981. Mafic silicates as indicators of intensive variables in granitic magmas: mining. Geology 31, 191–212.
Wones, D.R., Eugster, H.P., 1965. Stability of biotite: Experiment, theory and application. Am. Mineral. 50, 1228–1272.
Wu, J., Suppe, J., Lu, R., Kanda, R., 2016. Philippine Sea and East Asian plate tectonics since 52 Ma constrained by new subducted slab reconstruction methods. J. Geophys. Res. Solid Earth 121, 4670–4741. https://doi.org/10.1002/2016JB012923.
Xue, S., Ling, M.-X., Liu, Y.-L., Zhang, H., Sun, W., 2017. The genesis of early Carboniferous adakitic rocks at the southern margin of the Axla Block, North China. Lithos 278–281, 181–194.
Yumul Jr., G.P., 2007. Westward younging disposition of Philippine ophiolites and its implication for arc evolution. Isl. Arc 16, 306–317.
Yumul Jr., G.P., Brown, W.W., Dimalanta, C.B., Ausa, C.A., Faustino-Eslava, D.V., Payot, B.D., Ramos, N.T., Lizada, A.N., Buena, A.E., Villaplaza, B.R., Manalo, P.C., Queaño, K.L., Guotana, J.M.R., Pacle, N.A.D., 2017. Adakitic rocks in the Masara gold-silver mine, Compostela Valley, Mindanao, Philippines: different places, varying mechanisms? J. Asian Earth Sci. 142, 45–55.
Yumul Jr., G.P., Dimalanta, C.B., Bellon, H., Faustino, D.V., De Jesus, J.V., Tamayo Jr., R.A., Jumawan, F.T., 2000. Adakitic lavas in the Central Luzon back-arc region, Philippines: lower crust partial melting products? Isl. Arc 9, 499–512.
Yumul Jr., G.P., Dimalanta, C.B., Maglambayan, V.B., Marquez, E.J., 2008. Tectonic setting of a composite terrane: a review of the Philippine island arc system. Geosci. J. 12, 7–17.
Yumul Jr., G.P., Dimalanta, C.B., Tamayo Jr., R.A., Bellon, H., 2003a. Silicic arc volcanism in Central Luzon, the Philippines: characterization of its space, time and geochemical relationship. The Island Arc 12, 207–218.
Yumul Jr., G.P., Dimalanta, C.B., Tamayo Jr., R.A., Maury, R.C., 2003b. Collision, subduction and accretion events in the Philippines: a synthesis. The Island Arc 12, 77–91.
Yumul Jr., G.P., Dimalanta, C.B., Tamayo Jr., R.A., Zhou, M.F., 2006. Geology and geochemistry of the Rapu-Rapu Ophiolite Complex, eastern Philippines: possible fragment of the proto-Philippine Sea Plate. Int. Geol. Rev. 48, 329–348.
Zahirovic, S., Seton, M., Müller, R.D., 2014. The Cretaceous and Cenozoic tectonic evolution of Southeast Asia. Solid Earth 5, 227–273.
Zhang, J.-Q., Li, S.-R., Santosh, M., Wang, J.-Z., Li, Q., 2015. Mineral chemistry of high-Mg diorites and skarn in the Han-Xing iron deposits of South Taihang Mountains, China: constraints on mineralization process. Ore Geol. Rev. 64, 200–214.
Zhang, L., Li, S., Zhao, Q., 2019. A review of research on adakites. Int. Geol. Rev. https://doi.org/10.1080/00206814.2019.1702592.
Zhou, Z.X., 1986. The origin of intrusive mass in Fengshandong, Hubei Province. Acta Petrol. Sin. 29, 59–70 (in Chinese with English abstract).
Zhu, W.-G., Zhong, H., Chen, X., Huang, H.-Q., Bai, Z.-J., Yao, J.-H., Wang, Y.-J., Hu, P.-C., 2020. The earliest Jurassic A-type rhyolites and high-Mg andesites-dacites in southern Jiangxi Province, southeast China: evidence for delamination of a flat-slab. Lithos 358–359. https://doi.org/10.1016/j.lithos2020.105403.